Towards Cr(VI)-free anodization of aluminum alloys for aerospace adhesive bonding applications
A review

Abrahami, Shoshan T.; de Kok, John M.M.; Terryn, Herman; Mol, J.M.C.

Important note
To cite this publication, please use the final published version (if applicable).
Please check the document version above.

Towards Cr(VI)-free Anodization of Aluminum Alloys for Aerospace Adhesive Bonding Applications: A Review

Journal:	*Frontiers of Chemical Science and Engineering*
Manuscript ID	FCSE-2016-0181.R2
Manuscript Type:	Review
Date Submitted by the Author:	n/a
Complete List of Authors:	Abrahami, Shoshan; Technische Universiteit Delft, Materials Science and Engineering de Kok, John ; Fokker Technologies Terryn, Herman; Vrije Universiteit Brussel Mol, Johannes; Technische Universiteit Delft
Keywords:	Aluminium, Cr(VI)-free, Anodising, Adhesion
Speciality Area:	Sustainable technologies and green processing

SCHOLARONE™
Manuscripts

1   Front. Chem. Sci. Eng.

3   REVIEW ARTICLE

Towards Cr(VI)-free Anodization of Aluminum Alloys for Aerospace Adhesive Bonding Applications: A Review

6   Shoshan T. ABRAHAMI [1,2], John M.M. DE KOK [3], Herman TERRYN [2,4], Johannes M.C. MOL (□) [2]

7   1 *Materials innovation institute (M2i), Elektronicaweg 25, 2628 XG, Delft, The Netherlands*

8   2 *Delft University of Technology, Department of Materials Science and Engineering, Mekelweg 2, 2628*
9   *CD, Delft, The Netherlands*

10 3 *Fokker Aerostructures BV, Industrieweg 4, 3351 LB, Papendrecht, The Netherlands*

11 4 *Department of Materials and Chemistry, Research Group Electrochemical and Surface Engineering*
12 *(SURF), Vrije Universiteit Brussel, Pleinlaan 2, 1050 Brussels, Belgium*

13 © Higher Education Press and Springer-Verlag Berlin Heidelberg 2015

16 **Abstract**

17 For more than six decades, chromic acid anodizing (CAA) has been the central process in the surface
18 pre-treatment of aluminum for adhesively bonded aircraft structures. Unfortunately, this electrolyte
19 contains hexavalent chromium (Cr(VI)), a compound known for its toxicity and carcinogenic properties.
20 To comply with the new strict international regulations, the Cr(VI)-era will soon have to come to an end.
21 Anodizing aluminum in acid electrolytes produces a self-ordered porous oxide layer. Although different
22 acids can be used to create this type of structure, the excellent adhesion and corrosion resistance that is
23 currently achieved by the complete Cr(VI)-based process is not easily matched. This paper provides a
24 critical overview and appraisal of proposed alternatives to CAA, including combinations of multiple
25 anodizing steps, pre- and post anodizing treatments. The work is presented in terms of the modifications
26 to the oxide properties, such as morphological features (e.g. pore size, barrier layer thickness) and surface
27 chemistry, in order to evaluate the link between fundamental principles of adhesion and bond
28 performance.

31

1 Introduction

For many years, hexavalent chromium has been used for the corrosion protection of metals in many industries; aerospace, automotive, maritime and architectural structures are just a few examples for the wide spectrum of applications in which Cr(VI)-based coatings can guarantee the life-long integrity of metallic parts. Unfortunately, Cr(VI) is regarded to be extremely toxic and carcinogenic [1, 2]. This has already being noticed in the first decades of the 20th century [3, 4]. Numerous studies have shown that employees working with chromate-containing compounds risk exposure through skin contact and by inhalation of vapors or dust particles [5, 6]. In the aerospace industry this mostly occurs in the production stage, when the parts are pretreated and painted, during their maintenance or at the end-of life, when these coatings and paints are removed.

In 2006, the Occupational Safety and Health Administration (OSHA) in the U.S. [7], the European Registration, Evaluation, Authorization and Restriction of Chemicals (REACH, EC n°1907/2006) and Restriction of Hazardous Substancespolicies (RoHS) introduced new regulations that strictly limit the use of hexavalent chromium and announced its near future ban. As a consequence, chromates are no longer used in most commercial processes and products. However, the corrosion sensitivity of high-strength aluminum alloys and the required level of performance and safety make its overall replacement in the aerospace industry a very challenging task. In addition, the time it takes to test and qualify new systems for aviation is much longer compared to that in other industries. Therefore, Cr(VI)-based substances are currently still utilized in most aerospace metal pre-treatment, coating and bonding processes.

This paper reviews the state-of-the-art alternatives to *chromic acid anodizing* (CAA), which is the key pre-treatment step to produce anodic oxide films suitable for adhesive bonding. Herein, only the manufacturing of parts aimed for *structural* components are discussed. Although other components of the aircraft are produced in a similar manner, structural components are considered the most critical since they are designed as part of the principal load-carrying structure of the aircraft and they are typically not accessible for inspection and maintenance during its lifetime [8]. As such, these components are subject to the highest engineering standards.

The following section provides background on the main issues and challenges in the pre-treatments of aluminum for structural bonding. Next, section three presents the development of the benchmark CAA process that is currently used in Europe and its major oxide characteristics. The fourth section covers the range of Cr(VI)-free alternatives. In order to identify the key factors that determine the adhesion and durability of these structures, section five critically reviews the main processing parameters, as concluded by reviewing the literature available to date, including recent detailed investigations by the authors. The final section discusses the relation between the main oxide properties and bond performance. This review paper ends with a short summary and conclusion in section six.

2. Structural adhesive bonding in aircraft structures

Adhesive bonding is one of the oldest techniques to join different components, often of dissimilar nature [9]. Bonding is established when the adhesives undergoes physical or chemical hardening reaction (curing) to join the two panels together through surface adherence (adhesion) and internal strength (cohesion) [10]. Adhesive bonding was already used in the first aircrafts, which were made from wood

2

71   and continued in the 1940s, when manufacturers started using aluminum [11]. Since then adhesive
72   bonding has become a standard technique to produce the main body (fuselage), wings and other parts of
73   modern aircrafts [12]. Fig. 1 shows the main steps in the production of adhesively bonded components at
74   *Fokker Aerostructures* in the Netherlands.

75   **Figure 1** The production of metal-to-metal bonding at Fokker Aerostructures: (a) surface pre-treatment (panels hanging
76   above the anodizing bath), (b) parts drying on the rack after pre-treatment, (c) primer application, (d) adhesive application,
77   (e) a bonded part.

2.1 Durability of the adhesive bond

79   Ideally, the bonded structure will be able to withstand and carry the high loads that are executed on the
80   structure during use and efficiently transfer and distribute the mechanical stresses over a large surface
81   area. A crucial parameter in maintaining the long-term integrity of the assembly is durability of adhesion
82   under various environmental conditions, such as temperature extremes, varying atmospheric pressures,
83   moisture content and types of aggressive species (e.g. anti-freeze and chlorine ions). These, in
84   combination with the varying mechanical stresses, may lead to early failure [13]. Fig. 2 illustrates the
85   different possible failure mechanisms that can occur within an adhesive joint. They are generally
86   characterized as predominantly cohesive- or adhesive in nature. Cohesive failures take place within the
87   same phase, whereas adhesive failures occur at their interfaces.
88   Industrial standards generally demand higher adhesion than cohesion strengths. This is desired from an
89   engineering point of view, since cohesive failure related to bulk material properties could be readily
90   considered by design. In the case of metal-to-metal adhesive bonding, this refers to a cohesive failure
91   within the polymeric adhesive (Fig. 2 (A)). Other failure mechanisms (Fig. 2 (B)-(F)) are usually the
92   result of poor bond preparation (processing) and effects of environmental conditions.
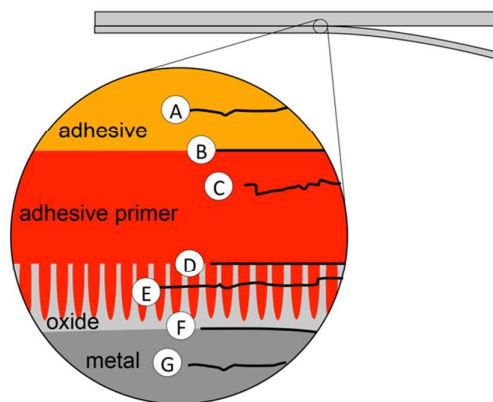
93

Figure 2 Schematic illustration of the possible failure modes in structural adhesive joint: (A) cohesive fracture of the adhesive film, (B) interfacial disbonding between adhesive and primer, (C) cohesive fracture of primer layer, (D) interfacial disbonding between primer and anodic coating, (E) fracture within anodic oxide coating and (F) corrosion of aluminum substrate at metal/oxide interface and (G) failure of the metal substrate.

One of the key issues concerning bond durability is the permeability of water molecules. Moisture from the environment can enter the bonded system by bulk diffusion through the adhesive, by interfacial diffusion along the interface between the adhesive and the oxide, and by capillary action through cracks or defects. Zanni-Deffarges and Shanahan [14] compared diffusion rates in bulk and bonded epoxy adhesive to show that capillary effects near the oxide-polymer interface can significantly enhance the diffusion rate of water in bonded joints. Once reaching the bond line, moisture can hydrate the oxide. This leads to the formation of oxyhydroxides, a weaker form of oxide with a larger volume [15]. Ultimately, this can lead to cohesive fracture within the hydrated oxide (Fig. 2 (E)). Alternatively, the presence of water at the interface can displace the previously formed bonds between the oxide and the resin, leading to delamination by de-adhesion (Fig. 2 (D)). Another dangerous failure mode is *bondline corrosion* (Fig. 2 (F)). It occurs when a relatively pure aluminum clad layer is present, which function as a sacrificial anode to the base materials. Also this type of failure is facilitated by the diffusion of water and other corrosion-initiating species (e.g. chlorine ions). Once bondline corrosion is initiated, it is characterized by disbonding at the interface followed by localized corrosion.

Pure aluminum metal has an inherent corrosion resistance due to the presence of a relatively uniform and thin oxide layer that protects the underlying metal [16]. This is caused by the high affinity of aluminum towards oxygen. Whenever the fresh metal surface is exposed to the atmosphere as, for example, in case of mechanical damage a new oxide layer will be formed. In dry conditions, this oxide film is typically a dense barrier layer of amorphous alumina (Al_2O_3) that is only 2 to 3 nm thick. In humid environments, this oxide will be covered by a more permeable hydrated aluminum hydroxide ($Al_2O_3 \cdot xH_2O$) at the outer surface. In that case the thickness of this layer can reach up to 10 nm [16]. These thin oxide layers are stable over a fairly broad range of pH ($4 < pH < 8.5$), providing aluminum with sufficient protection for various commercial purposes. At both lower and higher pH values this layer is not stable and it will dissolve [17].

Nevertheless, aluminum in aerospace applications is mainly used in its alloy form. The most commonly employed types of aluminum in the aerospace industry belong to the 2xxx and 7xxx alloy series. Within these families, AA2024-T3 and AA7075-T6 are the most used ones to date. The main alloying elements include copper (Cu), magnesium (Mg) and manganese (Mn) in AA2024 and zinc (Zn), magnesium (Mg),

4

127   copper (Cu) and silicon (Si) in AA7075. [18]. These heat-treatable alloys develop their strength by
128   precipitation hardening. As a consequence, the microstructure of these alloys is very complex, presenting
129   several second phase and intermetallic particles. The addition of alloying elements, though essential for
130   mechanical properties, can have detrimental consequences on to the substrate's corrosion resistance. The
131   electro potential differences between local areas of compositional differences can lead to galvanic
132   coupling and selective dissolution of the more active element. The most common type of corrosion in
133   aluminum alloys is pitting corrosion due to second phase particles in the matrix acting as cathodes or
134   grain boundary precipitation causing precipitate-free zones. These phenomena are especially pronounced
135   in AA2024-T3, which contains relatively high amounts of copper, a nobler element to aluminum. These
136   localized attacks can proceed to considerable depths within the substrate and may lead to grain fallout
137   when proceeding along grain boundaries. Detailed mechanisms of localized corrosion of AA2024-T3
138   under chloride conditions can be found elsewhere in the literature [19-21].

139   Additionally to their corrosion sensitivity, the surface of the substrate in its 'as-received' state is not
140   suitable for bonding. Metallurgical processing, including heat treatment and rolling, modifies the
141   uppermost layers of the alloy surface. Fig. 3 presents a schematic illustration of these layers, which
142   displays both compositional and structural changes, including smaller grains, enrichments in secondary
143   particles (dispersoids) and higher concentration of Mg and Zn [22]. Additionally, the high shear forces
144   applied during rolling are able to break and fold some of the surface oxides into the substrate. Altogether,
145   this result in a so-called 'near-surface deformed layers' (NSDL), which present significant different
146   electrochemical and mechanical properties compared to the bulk material. [23]. Hence, removing these
147   NSDL should be the first step in any type of further processing.

148   **Figure 3** Schematic illustration of the modified composition of the aluminum alloy surface present after metallurgical
149   processing [22].
150

3. Chromic acid anodizing (CAA)

152   In order to avoid the previously mentioned types of failure and to ensure long-term safety, bonded
153   metal-to-metal assemblies must be carefully prepared. Surface pre-treatment has emerged as the most
154   important step to provide the desired surface characteristics for bonding and minimize the effect of

5

155 surface heterogeneities, as the NSDL. The main pre-treatment schedule that is currently applied in the
156 aerospace industry is illustrated in Fig. 4. It consists of four major steps: degreasing, pickling (or
157 etching), anodizing, and primer application, all currently relying on Cr(VI)-based chemicals. In between
158 two subsequent steps the surface is thoroughly rinsed in water. The following subsections describe each
159 step of this pre-treatment scheme in terms of how it modifies the surface properties and its historical
160 context.

| As received Al alloy | Degreasing incl. $Na_2Cr_2O_7$ | Pickling with acids + CrO_3/ $Na_2Cr_2O_7$ | Chromic acid anodizing (CAA) | Primer with $SrCrO_4$ |

Processing time →

161 **Figure 4** schematic representations of the process steps and the modifications that take place during the complete Cr-based
162 pre-treatment that is currently applied in the European aerospace industry.

163

164 **Degreasing** is the first step in the pre-treatment process and normally the minimum preparation that is
165 carried out prior to any type of metal bonding. Degreasing removes any oils, grease and contaminations
166 that might have been introduced during aluminum manufacturing and processing [24]. This preliminary
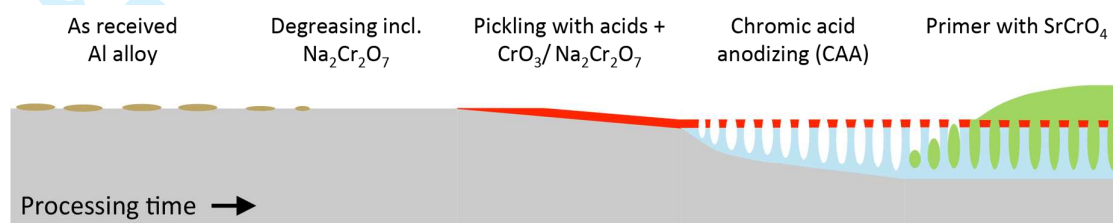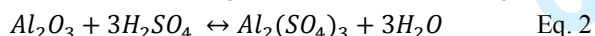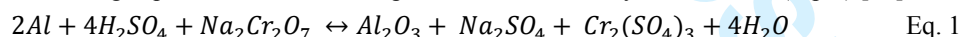167 cleaning is necessary to assure that the following steps will work evenly across the substrate surface [16].
168 Next, the modified surface layers are chemically removed by **pickling** (also called etching). This can be
169 performed in either acidic or alkaline solutions. The classical pickling solutions are often composed from
170 mixtures of chromic and sulfuric acids and they are generally divided into two types: the FPL- and the
171 CSA etch [25]. The first is the *Forest Products Laboratory* (FPL) process that was developed in the
172 1950s in the U.S. It consists of immersing the substrate in sodium dichromate ($Na_2Cr_2O_7$) and sulfuric
173 acid solution for 9-15 min at 65°C. The European version of this etch, the CSA pickling, uses lower
174 concentrations of either chromium trioxide (CrO_3) or sodium dichromate ($Na_2Cr_2O_7$) with sulfuric acid at
175 similar temperatures, but longer immersion times (30 min.) [26]. Both methods follow a two-step
176 reaction mechanism. In the first step, hexavalent chromium catalyses the oxidation of aluminum to
177 alumina following Eq. 1. Next, the alumina product is dissolved by sulfuric acid (Eq. 2) [16].

178 $$2Al + 4H_2SO_4 + Na_2Cr_2O_7 \leftrightarrow Al_2O_3 + Na_2SO_4 + Cr_2(SO_4)_3 + 4H_2O \qquad \text{Eq. 1}$$
179 $$Al_2O_3 + 3H_2SO_4 \leftrightarrow Al_2(SO_4)_3 + 3H_2O \qquad \text{Eq. 2}$$

180 Since the second step is slower than the first one, a thin oxide layer is produced on the surface (as
181 indicated by the red layer in Fig. 4). This oxide is amorphous, with a composition corresponding to
182 alumina (Al_2O_3) and some minor concentrations (~0.5%) of Cr and S impurities. Venables et al. [27]
183 reported that due to surface energy interactions, whiskers-like protrusions extending from the triple grain
184 boundary points extend up to 40 nm from the surface. In their paper, the authors suggest that these
185 branched protrusions already provide sufficient interlocking with the adhesive surface, resulting in an
186 improved adhesion.
187 Unfortunately, some early in-service failures (mostly of non-bonded structures) occurred in the
188 beginning of the 1960s, as aircrafts manufacturers started using epoxy adhesives instead of phenols [26].
189 The relatively thin oxide film was thus insufficient to provide reproducible and durable bonds.
190 Consequently, an extra step, anodizing, was added to the pre-treatment schedule. **Anodizing** is an
191 electrochemical process in which the aluminum substrate is artificially oxidized to grow a thick oxide
192 film (up to several μm) [16]. The process derives its name from the fact that the aluminum substrate is

6

193 used as the anode in an electrolytic cell. The anode (substrate) is connected to the positive terminal of a
194 DC power supply while a cathode (e.g. Al, stainless steel) is connected to the negative terminal. When
195 the circuit is closed, electrons are withdrawn from the aluminum anode, which facilitate the oxidation of
196 aluminum atoms to aluminum cations (Al^{3+}) at the metal/oxide interface. This is illustrated in Fig. 5.
197 Since the electronic conductivity of aluminum oxide is very low, the anodizing voltage that is applied on
198 the anodic cell encounters a resistance by the existing (natural) oxide film. This leads to a potential drop
199 over the metal/electrolyte interface, which give rise to high electric field over the oxide layer. These
200 electric fields are typically in the order of 10^6 to 10^7 V/m [28], which is high enough to enable oxide
201 growth by ionic migration through the oxide [29]. Since aluminum is anodized in an aqueous electrolyte,
202 adsorbed water at the anode will break down forming negatively charged O^{2-} and OH^-. These anions
203 migrate towards the positively charged anodic substrate. A reaction between Al^{3+} and O^{2-} will leads to
204 the formation of alumina, Al_2O_3, at the metal/oxide interface. Since not all the produced Al^{3+} is
205 consumed by this interface, excess Al^{3+} cations will migrate away from the positively charged anode.
206 Upon reaching the oxide/electrolyte interface, Al^{3+} can react with available O^{2-} forming additional
207 alumina at the oxide/electrolyte interface. Under certain conditions, alumina ions will be directly ejected
208 into the electrolyte. The conversion efficiency and, hence, final film morphology will depend on the
209 balance between oxide growth and oxide dissolution (through direct ejection and chemical attack by an
210 aggressive electrolyte). This in turn, is determined by the nature of the electrolyte and the process
211 conditions, as discussed later.

212
213
214
215
216
217
218
219
220

221 **Figure 5** Schematic representation of the aluminum/electrolyte interface, showing the ionic processes involved in oxide
222 growth during anodizing [30].

223 Chromic acid anodizing (CAA) was incorporated into the pre-treatment schedule in the 1960s. It mainly
224 aimed to improve the overall corrosion resistance by producing a thicker physical barrier between the
225 metal and its environment. Although anodizing can produce barrier- and porous-type oxide
226 morphologies, porous films are preferred for bonding purposes. As illustrated in Fig. 6, porous anodic
227 oxides consist of a compact barrier layer on the bottom and a relatively regular hexagonal porous
228 structure on top [31-34]. These films are created when the anodic oxide is sparingly soluble in the
229 anodizing electrolyte [31, 35]. In Europe, the 40/50V Bengough-Stuart process was adapted, using
230 2.5-3.0 wt.% chromic acid (CrO_3) at 40 °C [36]. The voltage across the electrolytic bath is initially raised
231 to 40V in the first 10 minutes. This voltage is then maintained for 20 more minutes before it is raised to
232 50V, where it is kept constant during the last 5 minutes [37]. The higher voltage at the end results in a
233 thicker barrier layer, providing an extra thick barrier for corrosive species [38].
234

This process produces 3-4 μm thick oxide layers on both AA2024-T3 and AA7075-T6 (bare and clad). It is a relatively ductile oxide with very low (0.1-0.3 wt.%) chromium content in the oxide. The oxide is moderately resistant to attack by moisture, although hydration has been reported [24]. This treatment, combined with prior CSA etching, was soon established as an effective pre-treatment for adhesive bonding and become an industrial standard.

In regular manufacturing operations, a certain time interval (several hours up to several months) usually passes between substrate pre-treatment and bonding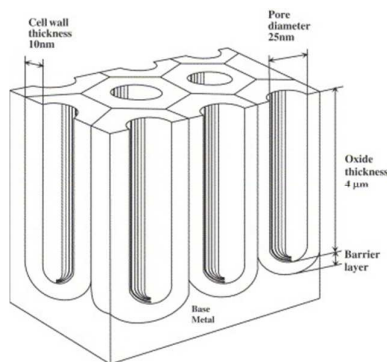. During this time, the freshly prepared oxide is susceptible to damage, contaminations, and environmental degradation [39]. This is prevented by the application of a thin layer of **primer** to seal the oxide immediately (within two hours) after the pre-treatments, when surface activity is maximal. Primers are diluted polymeric coatings, usually matching the chemistry of the adhesive. The primer functions as a physical barrier between the pretreated surface and its surrounding. Except for surface protection, primers are also used to promote adhesion. Two contributing mechanisms can be distinguished; (1) improved surface wetting and (2) providing stronger chemical interactions. The first mechanism is driven by the primer's lower viscosity (compared to the adhesive) and the addition of wetting agents. Kinloch et al, [40] compared PAA films that were bonded with- and without primer to show that a primer is able to penetrate deep and completely fill the pores, providing better adhesion. The second mechanism uses coupling agents to form a covalent bond across the inorganic-organic interface. Coupling agents are molecules with dual functionality. They contain organic end- groups such as methoxy (CH_3O-), ethoxy (CH_3CH_2O-) or hydroxyl (HO-) attached to a metallic central atom (e.g. silicon, zirconium or titanium) [41]. Organosilane coupling agents are the predominant chemical type of adhesion promoters. These groups are able to adsorb on the metal oxide surface through hydrogen bonds. Upon curing, a metallosiloxane bonds (Al-O-Si) are formed with the surface oxide [42]. These covalent bonds are much stronger than hydrogen bonds. Any remaining silanol groups will condense with themselves, forming a dense Si-O-Si network. Since Al-O-Si bond can be hydrolysed, the durability of these bonds will be determined by the extent of cross-linking of the Si-O-Si bonds, which will determine the hydrophobicity of the covering siloxane film. Hence, adjusting the chemical composition to tailor the desired film properties is essential. It is important to also match the reactivity of the coupling agent with that of the adhesive [41]. Different studies have demonstrated that silanes are capable to improve interfacial adhesion [40, 43-45], as well as corrosion resistance of coated aluminum [46, 47]. Song and van Ooij [48], for example, have shown that by combining two types of silanes, namely 1,2-bis(triethoxysilyl)ethane (BTSE) and ϒ-aminopropyltriethoxy (ϒ-APS), it is possible

8

269 to design a dual functionality interface that would give good corrosion protection and will be compatible
270 with an epoxy adhesive. Since silanes connect via the OH- groups on the substrate, maximizing their
271 amount on the substrate is desired. A study by Franquet et al. [49], showed that chemical pre-treatments
272 affecting the amount of surface hydroxyl groups will in turn affect the silane film uniformity and
273 thickness. Therefore, when silanes are applied, prior surface pre-treatment is still needed.

274 4. Cr(VI)-free alternatives to CAA

275 Health and environmental issues, together with the increasing costs associated with the treatment and
276 disposal of solutions containing hexavalent chromium initiated a large number of studies over the past
277 decades. To avoid an exhaustive comparison of the different process parameters, this section will focus
278 on the different methods rather than specific outcomes of the most relevant alternative Cr(VI)-free
279 pre-treatments for structural bonding. For a detailed list of the specific pre-treatments and evaluation
280 techniques, readers are encouraged to consult the review published by Critchlow and Brewis [24].

281 4.1 Phosphoric acid anodizing (PAA)

282 For economic reasons, anodizing was initially rejected in the US until Boeing introduced phosphoric acid
283 anodizing (PAA) in 1975, which makes PAA the first commercial alternative to CAA. The PAA process
284 applies 10wt.% phosphoric acid at 21-24 °C. Anodizing is conducted at constant voltage of 10-15 V for
285 25 minutes. The PAA oxide is considerably thinner (typically 0.5 to 2 μm) and more porous than the
286 CAA film [50]. However, it has an advantage, since the composition of the outer part of the film
287 corresponds to non-hydrated $AlPO_4$ in the outer layer (see section 5.2), which provides higher resistance
288 to humidity and even to hot water sealing. This resistance is attributed to the stability of the chemical
289 bonds between aluminum and phosphate [51] [52] and, therefore, provides an effective environmental
290 stability during service [53]. Nevertheless, studies show that the corrosion resistance of PAA oxides is
291 inferior to those of CAA, which explains why this process was developed together with the introduction
292 of chromate inhibiting primers. Hence, although the PAA process is Cr(VI)-free it typically requires the
293 additional support of (active) protective coatings that contain corrosion inhibitors. So far, the most
294 effective inhibitors are Cr(VI)-based pigments and the search for Cr(VI)-free alternatives is still in
295 progress. Some green inhibitors are based on inorganic species (including lithium, Cr(III), rare-earths,
296 molybdates and vanadates), while others are base on organic functionalities [54].

297 4.2 Mixed electrolytes anodizing

298 In addition to PAA, one of the most popular anodizing electrolytes is sulfuric acid. Conversely to PAA,
299 sulfuric acid anodizing (SAA) generally produces a thick and dens protective layer [55]. Therefore, SAA
300 is commercially applied (mostly in '*hard*' conditions) for decorative and corrosion protection
301 applications. However, the same properties that provides it with excellent corrosion and wear resistance
302 deliver poor adhesion [56]. One method to overcome this limitation is to mix sulfuric acid in the
303 anodizing bath with the more aggressive phosphoric acid, thereby providing the conditions to produce an
304 intermediate oxide structure with morphological dimensions comparable to CAA. The process, named
305 phosphoric-sulfuric acid anodizing (PSA) was developed by Kock et al. [57]. The first PSA process
306 contains equal amounts of sulfuric- and phosphoric acids (100 g/l). Similar to PAA, phosphates are found
307 in the outer layer of the oxide [58], providing an additional hydration resistance. Recent investigations by
308 the authors covered a broad range of process parameters: different concentrations of phosphoric and

9

309 sulfuric acids, together with ranging temperature and duration in the search for the optimal PSA
310 conditions [59]. Oxide films with wide morphological variations (e.g. pore size of 5 to 60 nm and layer
311 thicknesses of up to 6 μm) were prepared by changing the anodizing conditions (especially phosphoric
312 acid concentration and electrolyte temperature). These conditions were found important for the
313 performance of the bond, as tested by dry and wet floating roller peel tests. Currently, the PSA process is
314 considered a viable alternative to CAA and will be implemented at Fokker Aerostructures in the near
315 future.

316 Already in the 1960s, a mixture of tartaric and sulfuric acid anodizing (TSA) was suggested by Kape
317 [60]. Unfortunately, the resulting porosity is relatively low and adhesives cannot easily permeate into the
318 oxide layer. Hence, the analogous TSA process is mainly used in *non-structural* applications. The role of
319 tartaric acid, according to a study by Curioni et al. [61] is reducing the current density and thereby
320 reducing the oxide growth rate, so that the of the final film thickness is lower than for normal SAA. More
321 interestingly, however, an improved corrosion resistance is observed. This resistance is explained by a
322 "buffering effect" that tartarate ions remnants in the oxide are providing. During anodizing, tartaric acid
323 can combine with aluminum cations to produce aluminum tartrate, a compound that is highly soluble in
324 the acidic anodizing solution but with relatively low solubility in water. During subsequent rinsing, the
325 pH is rapidly increased and relatively large amounts of aluminum tartrate may precipitate at the pore
326 walls. As a consequence, if the oxide is exposed to a corrosive environment during its use, aluminum
327 tartrate may re-dissolve, producing a local buffer, thereby limiting the susceptibility to localized
328 corrosion. Even further improvements in the corrosion resistance of TSA films were registered after hot
329 water sealing [62] and by the addition of molybdate salts into the anodizing bath [63].

330 ## 4.3 Two-step anodizing

331 Relying on this TSA advantage, a new type of processes has emerged, which combines two-step
332 anodizing. In this case TSA anodizing follows PSA to provide a duplex oxide with both corrosion
333 resistance and adhesion capabilities. The resulting structure shown in Fig. 7 (a) is reported to be suitable
334 for adhesive bonding of structural components [64].

335

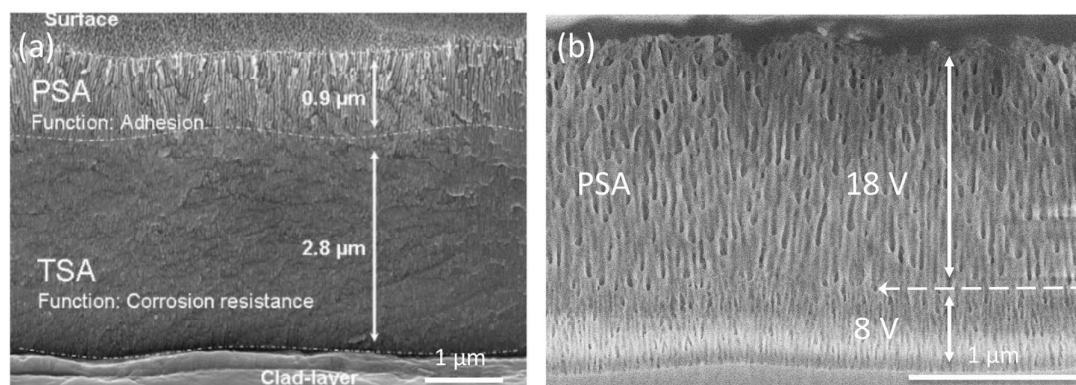336 **Figure 7** Cross section of the anodic oxide produced on 2024-T3 clad by (a) TSA+PSA process [64] and (b) PSA dynamic
337 anodizing, with voltage decrease from 18 V to 9 V [65].

338 Similar process is the boric-sulfuric acid anodizing (BSAA) that has been patented by Boeing as an
339 alternative to CAA [66]. The oxide structure resembles SAA, but with finer pores and more uniform

10

340   hexagonal arrangement compared to CAA, showing promising results [67]. Zhang et al. [68] report an
341   improvement in bonding and durability of panels created by the BSAA process by the addition of
342   phosphoric acid to the anodizing electrolyte. The process is reported to result in bigger pores, improving
343   primer penetration and extending oxide durability. Because boric acid is also hazardous, using it as a
344   replacement is not generally desired, especially since it may be subject to future regulations.

345   Similarly to two-step anodizing, dynamically changing the anodizing voltage/current during the process
346   can be used to vary the oxide morphology across its thickness. A SEM cross section of such an example
347   is shown in Fig. 7 (b), possibly providing an alternative for a two-step anodizing process. In an
348   investigation by van Put et al. [65] this complex oxide morphology was formed by an instantaneous
349   voltage decrease during anodizing. Since the pore size is linearly related to the applied voltage, an
350   instantaneous decrease from 18V to 9V forces the formation of new pores with smaller diameters below
351   existing larger pores. As a result, a distinct border between the two morphologies is formed (indicated by
352   the arrow in Fig. 7 (b)). Conversely, applying a voltage increase did not produce the reverse morphology
353   and a transition layer was formed by partly dissolving the walls of smaller pores after the sudden change.

354   ## 4.3 Electrolytic deoxidation

355   Earlier study by Venables et al. [27] have shown that fine oxide protrusions produced by the FPL etch on
356   top of a PAA oxide are beneficial for good adhesion. This is desired from adhesion point of view,
357   because protrusions, even just nanometers long, create an additional reinforcement by interlocking with
358   the resin. Likewise, Yendall and Critchlow [69] suggests a method that applies electrolytic phosphoric
359   acid deoxidizer (EPAD) before anodizing. In that respect EPAD replaces the FPL etch in producing an
360   open top layer that comes into contact with primer/adhesive (Fig. 8). They found that this method
361   improves the mechanical properties of the bond depending, however, also on the anodizing temperature
362   used for SAA. In this case, it is important to keep in mind that the choice of electrolyte and applied
363   temperature will also affect the resulting morphology. As discussed later in sections 5.1 and 5.4, if the
364   anodizing conditions are too aggressive, the EPAD layer may (in part or completely) dissolve during
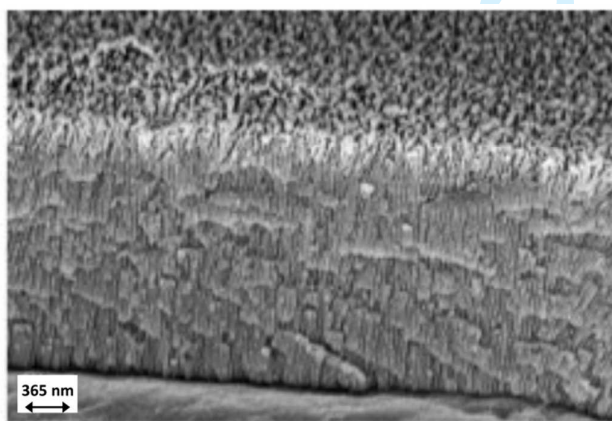365   subsequent anodizing.

366   **Figure 8** Cross section of AA2024-T3 clad after EPAD and SAA [69].

367   ## 4.4 AC Anodizing

11

368　An interesting alternative applies alternating current (AC) instead of the traditional direct current (DC)
369　for anodizing. AC anodizing was originally developed for high-speed coil applications in the automotive
370　industry [16]. Relatively elastic oxide layers are developed by treatment at higher temperatures and
371　higher anodizing currents. Both sulfuric- and phosphoric acid processes have been reported, with the
372　conditions listed in Table 1. Though developed as a continuous process, batch operation is also possible.

373

Table 1 Anodizing parameters [70].

Parameter	H_3PO_4	H_2SO_4
Acid concentration, wt.%	10	15
Temperature, °C	50	80
Time, min.	12	30
Current, A/dm^2	4	10

379　As in other AC processes, hydrogen evolves on the surface of the anode during the cathodic cycle. This
380　is sufficient to remove organic contaminants as well as natural present oxides, so that separate steps for
381　cleaning and deoxidizing prior to anodizing are not required, thereby drastically reducing the amount of
382　processing tanks [70]. Since the resulted oxides are thin, their performance is comparable to the etching
383　rather than anodic oxides [71]. Hence, a U.S. patent by Critchlow et al. [72] suggests applying a two-step
384　process that includes subsequent AC and DC PSA anodizing in the same bath. This combination
385　produces an oxide film that has a thin porous outer layer (less than 1 μm) and a relatively thick (up to 8
386　μm) uniform inner layer to yield an optimal combination of corrosion protection by the dense inner layer,
387　and adhesion provided by the porous outer layer.

388　4.5 Anodizing with post-treatments

389　Correspondingly, a post-treatment immersion of the relatively dense anodic oxide in a dilute acidic or
390　alkaline solution will produce the desired morphology by chemically attacking the oxide to partly
391　dissolve it and open the pores. Both Arrowsmith and Clifford [73] and Yendall and Critchlow [69]
392　applied phosphoric acid dip after SAA (or BSAA) anodizing to report an improved short and long-term
393　durability of the produced bonds. The narrow pores close to the substrate are considered to provide the
394　corrosion resistance, while the etched top layer is able to better interlock with the primer/adhesive. In
395　order to avoid over-etching, the time, nature and concentration of the etching solution should be
396　controlled [74]. Such post-anodizing step is not new to the aviation industry, which frequently applies
397　post- anodizing immersion in boiling water to seal the porous oxide layer when it serves as a protective
398　coating against corrosion instead of a receptive surface for bonding.

399　An interesting alternative to a post-treatment dip concerns anodizing combining positive and
400　small-negative voltages. The negative charge at the end of the normal anodizing cycle leads to
401　dissolution of the oxide by hydrogen ions attracted to the temporary negative pole [75]. In this case, the
402　dissolution is done in the same bath as anodizing, reducing the need for an extra processing and rinsing
403　bath.

404　4.6 Non-anodizing processes

12

405 As previously mentioned, immersion in hot water is often used to seal off the anodic pores. Treatment in
406 boiling water (and even water at 40 and 50 °C, [76]) leads to hydration of the present Al_2O_3 and to the
407 formation of a pseudoboehmite (AlOOH) oxide. Although sealing the pores openings is not desired from
408 a bonding perspective, boiling water treatment has been suggested as a stand-alone treatment to replace
409 anodizing. The hydrated form of oxide has been reported to provide many benefits, besides it being an
410 inexpensive alternative: a highly-porous morphology with a large surface area [77], increased number of
411 surface hydroxyl groups [78] and a low contact angle [79]. Oxide morphology will depend on the
412 temperature and the duration of the treatments. Three representative morphologies are presented in Fig.
413 9. After just 30 s of immersion the surface oxide exhibits a cellular structure with thin ridges (approx. 10
414 nm wide) that provide large porosity. As the treatment time is extended, cell walls develop into distinct
415 plates (of increased thickness) that are oriented normal to the surface. When the time is extended up to 4
416 hours, the cell walls significantly thickness, producing a distinctive and much less porous structure [80].
417 Unfortunately, this type of oxide is brittle and mechanical tests often show an early cohesive failure
418 within this pseudoboehmite layer [77, 79]. Although in some cases, the combination of prior grit blasting
419 and the addition of a silane layer was shown to reproduce results comparable to the benchmark used
420 (CSA+PAA), its level of success is highly sensitive to alloy composition [80]. Hence, boiling water
421 treatment generally does not compare with the durability of anodized-based oxide layers.

422 **Figure 9** High-resolution SEM micrograph after boiling water treatment on AA2024-T3 clad for 30 s (a), 60 min (b) and
423   240 min (c), edited from [80].

424 A similar option consists of a steam treatment [81, 82]. A study by Ud Din et al. [83] have shown that
425 oxide layers with thicknesses comparable to anodic oxides can be produced. Depending on treatment
426 parameters and steam chemistry, layers of few nanometers up to 3 μm can be formed. The addition of
427 acidic components (citric or phosphoric acids) to the steam enables the growth of thicker layers and help
428 in the corrosion protection (especially due to incorporation of phosphates).

429 ## 5. Parameters affecting the anodic oxide film properties

430 Considering the list of alternative methods in section 4, it appears that most processes are based on
431 similar electrolytes that apply different preparation conditions to produce certain desired oxide
432 properties. Hence, it is important to understand which key parameters control the anodizing process and
433 how these, in turn, change the oxide film characteristics.
434

435 ## 5.1 Electrolyte type

436 The nature of the electrolyte is one of the main parameters to determine the oxide properties, such as
437 morphology and chemistry (as discussed in section 5.2). The pore size is a direct function of the

13

438 electrolyte as found by Keller et al. [84]. Interpore distance and barrier layer thickness are also affected,
439 but to a lesser degree. The pore size generally increases in the order SAA < TSA < CAA< < PSA< PAA
440 [85].

441 ## 5.2 Incorporation of anions

442 Besides the ionic species (Al^{3+} and O^{2-}/OH^-) that are responsible for oxide growth, any ion species that is
443 present in the solution may be affected by the electric field. Since the anode is positively charged during
444 anodizing, negatively charged species from dissociating acids will migrate towards the oxide, leading to
445 the incorporation of impurities into the oxide. The extent of incorporation is determined by the nature of
446 the electrolyte solution, the applied conditions and the film type. A range of surface analysis techniques,
447 including Auger electron spectroscopy (AES), X-ray photoelectron spectroscopy (XPS) and glow
448 discharge optical emission spectroscopy (GDOES) [86, 87] have been applied to measure the
449 concentration and distribution of electrolyte-derived impurities in the film. These studies show that the
450 migration of electrolyte species varies from one electrolyte to the other. Table 2 lists the concentration of
451 anions within the most common anodizing electrolytes. It demonstrates that almost anion-free films are
452 formed in chromic acid, while other anions of alternative electrolytes contribute to a much higher relative
453 composition. Since most electrolyte anions migrate at slower rates than the O^{2-} ions, a relatively pure
454 alumina region is formed close to the aluminum/oxide interface [88]. This is indicated in Fig. 10 that
455 displays a comparison of the resulting oxide composition in SAA and PAA. Sulfate anions can migrate
456 into the inner most part of the cell wall, resulting in a duplex oxide composition. Phosphate anions, on
457 the other hand, exhibit a triplex structure with maximal concentration in the region near the interface
458 with the electrolyte. In the mixed PSA (Phosphoric- sulfuric acid anodizing) electrolyte, the
459 incorporation of phosphate on *barrier-type* oxide indicated that the phosphate incorporation in the mixed
460 electrolyte is somewhat inhibited, and phosphates remained close to the oxide/resin interface [58].

461
462

Table 2: Percentage of incorporated anions in the porous oxide layer [85].

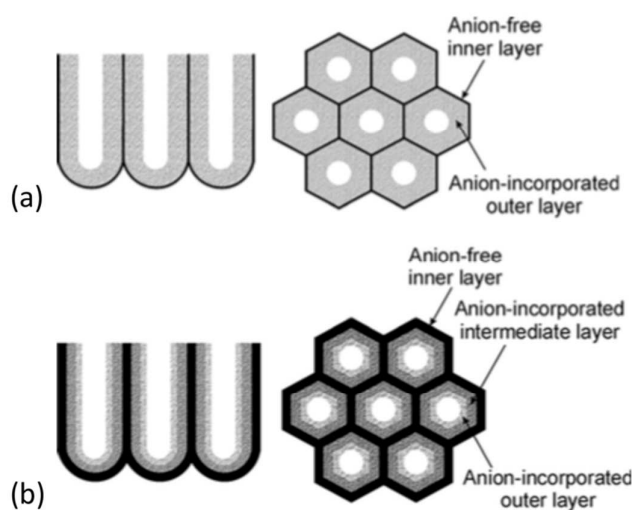| Electrolyte	H_2CrO_4	H_3PO_4	$H_2C_2O_4$	H_2SO_4
Anion concentration (at.%)	$0.1 - 0.3$	6 - 8	2 - 3	10 - 13

463
464 **Figure 10**: Schematic representations of the sectional and plan views of, respectively, the duplex (a) and triplex (b)
465 structures of porous alumina cell walls formed in sulfuric and phosphoric acids, respectively [85].

14

466 Compared to barrier layers, porous film generally contain a higher anion content in the oxide structure

467 [85]. This is explained by the fact that the electric field at the barrier layer is not uniform, so that the

468 semi-spherical shape of the pore base results in a much higher electric field close to the electrolyte/oxide

469 interface, which in turn supports easier incorporation of anions. In addition, the long-term exposure of

470 the oxide walls to the electrolyte readily allows for active penetration of the acid.

471 Anion incorporation has an effect on the properties of the oxide film, such as the mechanical (e.g.

472 flexibility and hardness) the chemical properties and the space charge [89]. Thompson and Wood [90]

473 reported a transition from solid to gel-like material moving across the cell walls towards the pore interior,

474 with the thickness of this layer depending on the electrolyte, the voltage or current density, and the

475 temperature. Another example is the resistance to hydration that is provided by oxides produced in

476 phosphoric acid. This resistance has been contributed to the presence of $H_2PO_4^-$ ions in the anodic films.

477 These anions can be further decomposed to proton, H^+, and HPO_4^{2-}, thereby retarding the hydration of

478 alumina [68]. The applied electrolyte also seems to have an influence on the water content of the film.

479 Although no water is found in the bulk of oxides formed in acid electrolytes, chemical adsorption

480 (chemisorption) of OH^- groups and water molecules at the outer layer is reported [91]. This can,

481 according to findings on chemically grown aluminum oxides, affect the extent in which the oxide interact

482 with organic molecules and resins [92].

483 In a recent publication by the authors [58] we have quantified the relative amount of O^{2-}, OH^-, PO_4^{3-} and

484 SO_4^{2-} species at the surface of *barrier-type* PAA, SAA, PSA and CAA oxides using X-ray photoelectron

485 spectroscopy (XPS). Results show that the surface chemistry of anodic oxides is highly affected by the

486 incorporation of anions. Phosphates were the highest with 40 % of the surface species and no hydroxyls

487 at the applied conditions. Sulfate concentration is lower at 15 % and a negligible amount of anions in

488 CAA. It was confirmed that the incorporation of phosphate and sulfate anions comes at the expense of

489 surface hydroxyls. Consequentially, we investigated how variations in the chemical species at the oxide

490 surface after anodizing affect the interaction with an organic resin. In the first instate, this was studied

491 using molecules that represent typical aerospace adhesives. Results show that bonding with two

492 phenol-based molecules and amine molecule both proceeds through the surface hydroxyls. However,

493 interactions with some molecules were sensitive to chemical changes while others did not. Next,

494 mechanical peel tests with barrier-type anodic oxides that were bonded with an industrial epoxy

495 adhesive. We concluded that the bonding mechanism was not affected by anion incorporation, only its

496 extent. Since phosphate and sulfate incorporation reduces the amount of hydroxyls available for

497 interactions, anodizing in these electrolytes was considered inferior from a chemical interactions point of

498 view [93].

499

5.3 Potential / current density

500

501 At steady state growth, a dynamic equilibrium exists between pore base dissolution at the

502 oxide/electrolyte interface and oxide growth at the metal/oxide interface. Studies have shown that the

503 major film characteristics (pore diameter *d*, cell diameter *c* and barrier layer thickness *b*, as indicated in

504 Fig. 11) are directly related to the applied potential [84, 94]. This is explained by the fact that stationary

505 film formation occurs at a constant rate, which is determined by the average field over the oxide [95].

506 Higher potential values will result in thicker barrier layers, larger cells, and wider pores. The thickening

507 of the barrier layer was found to show an almost universal relation, growing at 1.3-1.4 nm/V for

508 barrier-type films and about 1.2 nm/V for the barriers under porous films, with only small deviations as a
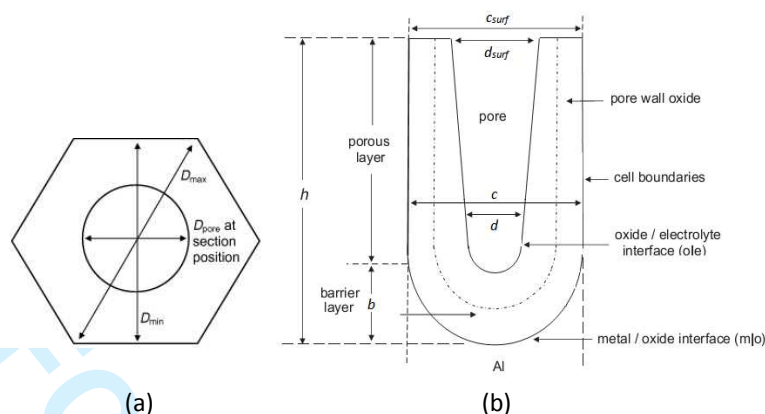509 function of the temperature and the electrolyte type [85].

(a) (b)

510 **Figure 11**: Schematic representation of an ideally hexagonal columnar cell of a porous anodic alumina film [95].
511

512 Any tendency of a pore to become too big or too small will be compensated by its curvature that will,
513 accordingly, adjust field strength [96]. If during the anodizing process, a large variation in potential is
514 induced, the oxide film will adapt itself to the new applied conditions. This observations, together with a
515 'recovery effect' was reported by Curioni et al. [97], using cyclic polarization measurements. The
516 recovery effect is the elapsed time before the steady-state characteristic conditions of the new voltage are
517 attained. It will depend on the potential variance, as well as the bath conditions (electrolyte, temperature).
518 Dynamically varying the anodizing potential during the treatment was used by van Put et al. [65] in order
519 to change the pore size across the oxide thickness, creating complex oxide morphologies. This may
520 explain the gradient of voltage that is applied during the conventional 40/50V CAA anodizing process,
521 providing wider pores at the bottom of the film and thickening the barrier layer. This is an interesting
522 observation that can be used as opportunity in developing new processes.
523

524 5.4 Temperature and time

525 Another significant variable in the anodizing conditions is the electrolyte temperature. A higher bath
526 temperature will enhance local dissolution at the pore base. This, in turn, will result in an increased local
527 current density, which will increase the ionic transfer and oxide formation rates [98]. Aerts et al. [99]
528 have shown that a higher rate of oxide dissolution, due to the aggressiveness of the electrolyte at higher
529 temperatures, have increased the porosity in sulfuric acid anodizing (with a constant convection) from
530 4% at 5 ℃ to 32% at 55 ℃. Dissolution effects are mainly noticeable at the outer layer of the oxide,
531 leading to pore broadening [100]. Upon extended anodizing times, aggressive electrolytes will cause
532 excessive chemical dissolution. Since the oxide is only growing from within the metal, the outer part of
533 the film is in contact with the electrolyte for a longer time period and therefore suffers from the most
534 chemical attack. This phenomenon induces pore widening at the outer surface, which affects the general
535 shape of the pores. This is why cone-shaped pores are often reported; with the pore diameter at the pore
536 base (d in Fig. 11 (b)) generally exhibiting a linear correlation to the anodizing voltage, while pores at the
537 surface (d_{surf} in Fig. 11 (b)) are frequently larger [59]. Interestingly, controlling the electrode temperature
538 can have a larger influence on oxide formation than changing the electrolyte temperature [101]. Hence,
539 physical bath properties, such as convection-based heat transfer should be considered.

16

540 At high anodizing temperatures and longer times, dissolution has an even larger influence on oxide
541 morphology. An example is shown in Fig. 12 for different electrolyte temperatures and dwell time. At
542 relatively lower temperatures and shorter times whiskers are formed on top of the hexagonal oxide
543 structure. These are created by extended dissolution and thinning of the pore walls. At some critical
544 point, these filaments are so long and thin, that they will collapse, forming a so-called 'bird's nest'
545 structure on top of the oxide film (Fig. 12 m-o).
546

547
548 **Figure 12:** SEM of the oxide layer depending on the bath temperature and the dwell time - surface views (anodizing
549 potential E = 50 VSCE) [102]. Longer time and higher temperatures lead to their collapse and the formation of a 'bird's
550 nest'.
551

552 ## 5.5 Pre-texturing

553 Studies have shown that surface features produced by prior steps are related to pore initiation and
554 development. Following the previously discussed growth mechanism, geometrical (near-)surface features
555 like the rolling lines, scratches and rolled-in oxides locally increase the curvature and therefore present
556 preferential regions for pore initiation and development. It has been shown by Terryn [103] that such
557 features can even pre-impose the alignment of pores to develop certain orientation. This is especially
558 relevant when the step prior to anodizing produces characteristic surface features. If a highly-regular pore
559 arrangement is required, as in the production of alumina template for nanostructure fabrication, a
560 two-step anodizing (with intermediate dissolution of the oxide) is used to produce a well-ordered
561 structure, in which the first anodizing step is used to texture the surface [85]. Since this method is both
562 time-consuming and expensive, pre-texturing by anodizing is generally not applied in the aerospace
563 industry.

564 ## 5.6 Alloy composition

565 The presence of alloying elements has an effect on the anodizing potential, as well as the oxide
566 morphology. Since elements in solid solution will change the resistance to current flow, the purer the
567 aluminum, the more resistance to ionic transport [104].

17

568 It is generally also observed that the same process conditions can yield completely different forms of
569 anodic films on bare and clad aluminum substrates. Fig. 13 shows a comparison between the CAA
570 40/50V anodic oxide on clad and bare AA20204-T3. The high purity clad alloy shows a relatively
571 regular columnar structure while no evidently regular structure is observed on the bare material, which
572 resembles a sponge-like structure. This difference is attributed to the presence of second phase particles
573 and alloying elements with a different potential than that of the matrix [69, 105, 106]. Alloying elements
574 with more negative potential will oxidize with aluminum and enter the anodic oxide, while nobler
575 alloying elements like Cu do not. Cu concentration will then rise, leading to enrichment at the
576 metal/oxide interface, immediately beneath the oxide film [107, 108]. It has been shown by
577 Garcia-Vergara et.al [109] that cyclic oxidation of copper in the enriched layer below the barrier layer
578 results in oxygen generation that leads to gas evolution and lateral porosity, resulting in the irregular
579 anodic oxide structure that is produced on bare A2024-T3. Correspondingly, similar process conditions
580 may lead to different oxide weight and morphology on different aluminum alloys.

581 **Figure 13**: CAA 40/50 V processed, 2024-T3 bare: plan view (a) and cross-section (b), 2024-T3 clad: plan view (c) and
582 cross-section (d). Reprinted from [69], Copyright (2016), with permission from Elsevier.

583 # 6. The relation between oxide properties and adhesion

584 The two main oxide properties that are influenced by the different process parameters are oxide
585 composition and morphological features. Yet, it appears that the main objective in the development of
586 Cr(VI)-free processes so far was to reproduce the CAA morphological features using different types of
587 processes. One of the longest, yet, on-going discussions in the literature concern the adhesion modes.
588 Various theories exist to explain adhesion between different materials: diffusion, electrostatic
589 interactions, weak boundary layer, mechanical interlocking and physical chemical adsorption (or
590 interactions) [110]. Amongst these theories adsorption and mechanical models are considered most
591 relevant for metal/polymer bonding.

592 Different authors argue that the high level adhesion that is achieved with porous anodic oxides is mainly
593 due to mechanical interlocking [27, 111-113]. However, studies on both chemical and anodic oxides
594 have shown that oxide chemistry also plays a vital role in the nature and type of interaction with the
595 organic resin [92, 114-117]. In an effort to separate the two contributions, a study by the authors using

18

596 FM 73 epoxy adhesive shows that significant initial adhesion strength can be achieved without
597 mechanical interlocking and independent of the type of electrolyte. The measured dry peel strengths were
598 in the same level of the dry strengths measured for porous oxides with a relatively small pore size (up to
599 20 nm). However, porous oxides with wider pores performed better. Above approximately 25 nm pore
600 size, tests showed no further improvement in dry peel strengths [59]. According to these observations, it
601 is not possible to conclude which is the dominating adhesion mechanism. Both mechanical interlocking
602 and a larger contact area could provide this improvement in strength.

603 Conversely, the stability of the interface under water ingress was found to be highly dependent on the
604 oxide chemistry and anodizing conditions, especially the electrolyte type, concentration and temperature.
605 Chemistry effects were correlated to the amount of surface hydroxyls, which were found to be the
606 reacting entities between the oxide and the resin [116], while morphological considerations were mainly
607 attributed to changes in the surface roughness [59]. Nevertheless, bond strength and durability both
608 appear to be closely related to the ability of the oxide and the resin to form a cohesive interphase.
609 Although mechanical interlocking is considered to contribute, there is no conclusive evidence for its
610 dominance.

611 Another important aspect in bond durability is the resistance to bondline corrosion. It appears that
612 increasing the oxide porosity and surface roughness will improve adhesion. However, as also claimed to
613 PAA, one of the main challenges is to provide a high level of corrosion resistance in a very porous
614 system. Consequently, failures due to bondline corrosion were observed with PSA test panels produced
615 at relatively aggressive conditions and lower voltages [59]. Oxides produced in the same conditions
616 (electrolyte, temperature and time), but at higher voltage did not fail. This seems to indicate that the
617 presence of thicker barrier-layer that is formed at higher voltages may be playing a significant role.
618 Furthermore, this is the reason why many studies combine the production of a receptive open structure at
619 the outer layer, while aiming to provide better corrosion protection by a denser inner layer. Nevertheless,
620 a recent (unpublished) investigation of the authors indicates that the corrosion resistance of the interface
621 is also largely determined by the chemical composition of the adhesive. Hence, the chemical nature of
622 the oxide *and* the adhesive should be considered.

623 ## 7. Summary and Conclusions

624 The required bond performance and durability, together with the corrosion sensitivity of aerospace
625 aluminum alloys, have led to the development of a multi-step pre-treatment process that is carefully
626 designed to provide the desired surface characteristics for bonding and corrosion resistance. In this
627 pre-treatment, the use of Cr(VI)-based chemistries currently still has a crucial role. The importance of
628 finding a replacement is evident by the large amount of literature available on this subject. It is, however,
629 also clear that the success and versatility of Cr(VI)-based applications is one that is very difficult to
630 duplicate. While many Cr(VI)-free alternative options exist and much is known about the relation
631 between the principal process parameters and oxide properties, maximizing bond performance and
632 corrosion resistance is not straightforward. The fact that both atomic- and molecular interactions, as well
633 as mechanical interlocking are crucial for the formation of interfacial bonds are now beginning to be
634 reflected in practical and industrial research. Hence, it is of pivotal importance to adjust both oxide
635 chemistry and morphology in order to produce the desired oxide characteristics. It remains of great
636 academic and industrial interest to continue to gain further fundamental understanding on how adsorption
637 and mechanical adhesion mechanisms contribute to the final bond performance.

19

8.References

1. ATSDR. Toxicologica Profile for Chromium. 2012,

2. Sueker J K. 5 - Chromium A2 - Morrison, Robert D. In: Murphy B L, (ed). Environmental Forensics. Burlington: Academic Press, 1964, 81-95

3. Royle H. Toxicity of chromic acid in the chromium plating industry (1). Environmental Research, 1975, 10(1): 39-53

4. Murray R. Health of Workers in Chromate Producing Industry. British Journal of Industrial Medicine, 1957, 14(2): 140-141

5. Alexander B H, Checkoway H, Wechsler L, Heyer N J, Muhm J M, O'Keeffe T P. Lung Cancer in Chromate-Exposed Aerospace Workers. Journal of Occupational and Environmental Medicine, 1996, 38(12): 1253-1258

6. Vallero D. Chapter 11 - Cancer and Air Pollutants. Fundamentals of Air Pollution (Fifth Edition). Boston: Academic Press, 2014, 271-311

7. OSHA. Toxic and Hazardous Substances Occupational Exposure to Hexavalent Chromium, 2006, 1910.1026(

8. Ebnesajjad S. 1 - Introduction and Adhesion Theories. In: Ebnesajjad S, (ed). Handbook of Adhesives and Surface Preparation. Oxford: William Andrew Publishing, 2011, 3-13

9. Brockmann W, Geiß P L, Klingen J, Schröder B. Adhesive Bonding: Wiley-VCH Verlag GmbH & Co. KGaA, 2009

10. Marshall S J, Bayne S C, Baier R, Tomsia A P, Marshall G W. A review of adhesion science. Dental Materials, 2010, 26(2): e11-e16

11. Bishopp J. Adhesives for Aerospace Structures. In: Ebnesajjad S, (ed). Handbook of Adhesives and Surface Preparation. Oxford: William Andrew Publishing, 2011, 301-344

12. Higgins A. Adhesive bonding of aircraft structures. International Journal of Adhesion and Adhesives, 2000, 20(5): 367-376

13. Sargent J P. Durability studies for aerospace applications using peel and wedge tests. International Journal of Adhesion and Adhesives, 2005, 25(3): 247-256

14. Zanni-Deffarges M P, Shanahan M E R. Diffusion of water into an epoxy adhesive: comparison between bulk behaviour and adhesive joints. International Journal of Adhesion and Adhesives, 1995, 15(3): 137-142

15. Posner R, Ozcan O, Grundmeier G. Water and Ions at Polymer/Metal Interfaces. In: Silva M L F, Sato C, (eds). Design of Adhesive Joints Under Humid Conditions. Berlin, Heidelberg: Springer Berlin Heidelberg, 2013, 21-52

16. Sheasby P G, Pinner R. Surface Treatment and Finishing of Aluminium and its Alloys. 6th ed. England: Finishing Publications Ltd., 2001.

17. Sukiman N L, Zhou X, Birbilis N, Hughes A E, Mol J M C, Garcia S J, X. Z, Thompson G E. Durability and Corrosion of Aluminium and Its Alloys: Overview, Property Space, Techniques and Developments. Aluminium Alloys - New Trends in Fabrication and Applications: InTech, 2012, 47- 97

18. Lyle J P, Granger D A, Sanders R E. Aluminum Alloys. Ullmann's Encyclopedia of Industrial Chemistry: Wiley-VCH Verlag GmbH & Co. KGaA, 2000

19. Boag A, Hughes A E, Glenn A M, Muster T H, McCulloch D. Corrosion of AA2024-T3 Part I: Localised corrosion of isolated IM particles. Corrosion Science, 2011, 53(1): 17-26

20. Hughes A E, Boag A, Glenn A M, McCulloch D, Muster T H, Ryan C, Luo C, Zhou X, Thompson G E. Corrosion of AA2024-T3 Part II: Co-operative corrosion. Corrosion Science, 2011, 53(1): 27-39

20

683   21.   Glenn A M, Muster T H, Luo C, Zhou X, Thompson G E, Boag A, Hughes A E. Corrosion of
684   AA2024-T3 Part III: Propagation. Corrosion Science, 2011, 53(1): 40-50
685   22.   Afseth A. Norway: NTNU Trondheim, 1999
686   23.   Zhou X, Liu Y, Thompson G E, Scamans G M, Skeldon P, Hunter J A. Near-Surface
687   Deformed Layers on Rolled Aluminum Alloys. Metallurgical and Materials Transactions A, 2011, 42(5):
688   1373-1385
689   24.   Critchlow G W, Brewis D M. Review of surface pretreatments for aluminium alloys.
690   International Journal of Adhesion and Adhesives, 1996, 16(4): 255-275
691   25.   Wegman R F, Van Twisk J. 2 - Aluminum and Aluminum Alloys. In: Wegman R F, Twisk J
692   V, (eds). Surface Preparation Techniques for Adhesive Bonding (Second Edition): William Andrew
693   Publishing, 2013, 9-37
694   26.   Pocius A V. The Electrochemistry of the FPL (Forest Products Laboratory) Process and its
695   Relationship to the Durability of Structural Adhesive Bonds. The Journal of Adhesion, 1992, 39(2-3): 101-121
696   27.   Venables J D, McNamara D K, Chen J M, Sun T S, Hopping R L. Oxide morphologies on
697   aluminum prepared for adhesive bonding. Applications of Surface Science, 1979, 3(1): 88-98
698   28.   Carter E A. High current anodization of magnesium and magnesium alloysThe University of
699   Auckland, 1996
700   29.   Su Z, Zhou W. Porous Anodic Metal Oxides. Science Foundation in China, 2008, 16(1): 36
701   30.   Aerts T. Study of the influence of temperature and heat transfer during anodic oxide growth on
702   aluminiumVrije Universiteit Brussel, 2009
703   31.   Thompson G E. Porous anodic alumina: fabrication, characterization and applications. Thin
704   Solid Films, 1997, 297: 192-201
705   32.   O'Sullivan J P, Wood G C. Morphology and mechanism of formation of porous anodic films
706   on aluminum. Proceedings of the Royal Society of London Series A - Mathematical and Physical Sciences,
707   1970, 317: 511-543
708   33.   Setoh S, Miyata A. Sci. Pap. Inst. Phys. Chem. Res., 1932, 189
709   34.   Keller F, Hunter M S, Robinson D L. Structureal features of oxide coatings on aluminum.
710   Journal of The Electrochemical Society, 1953, 100: 411-419
711   35.   Wernick S, Pinner R, Sheasby P G. The surface treatment and finishing of aluminium and its
712   alloys. 5 ed. Ohio and Middlesex: ASM International and Finishing Publications LTD., 1987
713   36.   Critchlow G W, Yendall K A, Bahrani D, Quinn A, Andrews F. Strategies for the replacement
714   of chromic acid anodising for the structural bonding of aluminium alloys. International Journal of Adhesion
715   and Adhesives, 2006, 26(6): 419-453
716   37.   Brockmann W, Hennemann O D, Kollek H. Surface properties and adhesion in bonding
717   aluminium alloys by adhesives. International Journal of Adhesion and Adhesives, 1982, 2(1): 33-40
718   38.   Oosting R. Toward a new durable and environmentally compliant adhesive bonding process
719   for aluminum alloys. The Netherlands Delft University of Technology, 1995
720   39.   Olsson-Jacques C L, Wilson A R, Rider A N, Arnott D R. Effect of Contaminant on the
721   Durability of Epoxy Adhesive Bonds with Alclad 2024 Aluminium Alloy Adherends. Surface and Interface
722   Analysis, 1996, 24(9): 569-577
723   40.   Kinloch A J, Little M S G, Watts J F. The role of the interphase in the environmental failure of
724   adhesive joints. Acta Materialia, 2000, 48(18–19): 4543-4553
725   41.   G. Pape P. 15 - Adhesion Promoters. In: Ebnesajjad S, (ed). Handbook of Adhesives and
726   Surface Preparation. Oxford: William Andrew Publishing, 2011, 369-386

21

727   42.   Abel M-L, Digby R P, Fletcher I W, Watts J F. Evidence of specific interaction between
728   γ-glycidoxypropyltrimethoxysilane and oxidized aluminium using high-mass resolution ToF-SIMS. Surface
729   and Interface Analysis, 2000, 29(2): 115-125
730   43.   Tchoquessi Doidjo M R, Belec L, Aragon E, Joliff Y, Lanarde L, Meyer M, Bonnaudet M,
731   Perrin F X. Influence of silane-based treatment on adherence and wet durability of fusion bonded epoxy/steel
732   joints. Progress in Organic Coatings, 2013, 76(12): 1765-1772
733   44.   Ooij W, Zhu D, Palanivel V, Lamar J A, Stacy M. Overview: The Potential of silanes for
734   chromate replacement in metal finishing industries. Silicon Chemistry, 2006, 3(1-2): 11-30
735   45.   Thiedmanu W, Tolan F C, Pearce P J, Morris C E M. Silane Coupling Agents as Adhesion
736   Promoters for Aerospace Structural Film Adhesives. The Journal of Adhesion, 1987, 22(3): 197-210
737   46.   Cabral A, Duarte R G, Montemor M F, Zheludkevich M L, Ferreira M G S. Analytical
738   characterisation and corrosion behaviour of bis-[triethoxysilylpropyl]tetrasulphide pre-treated AA2024-T3.
739   Corrosion Science, 2005, 47(3): 869-881
740   47.   Cabral A M, Duarte R G, Montemor M F, Ferreira M G S. A comparative study on the
741   corrosion resistance of AA2024-T3 substrates pre-treated with different silane solutions: Composition of the
742   films formed. Progress in Organic Coatings, 2005, 54(4): 322-331
743   48.   Song J, Van Ooij W J. Bonding and corrosion protection mechanisms of γ-APS and BTSE
744   silane films on aluminum substrates. Journal of Adhesion Science and Technology, 2003, 17(16): 2191-2221
745   49.   Franquet A, Terryn H, Vereecken J. Study of the effect of different aluminium surface
746   pretreatments on the deposition of thin non-functional silane coatings. Surface and Interface Analysis, 2004,
747   36(8): 681-684
748   50.   Park S Y, Choi W J, Choi H S, Kwon H, Kim S H. Recent Trends in Surface Treatment
749   Technologies for Airframe Adhesive Bonding Processing: A Review (1995–2008). The Journal of Adhesion,
750   2010, 86(2): 192-221
751   51.   Hughes A E, Cole I S, Muster T H, Varley R J. Designing green, self-healing coatings for
752   metal protection. NPG Asia Mater, 2010, 2: 143-151
753   52.   Marceau J A, Firminhac R H, Moji Y. Method for providing environmentally stable aluminum
754   surfaces for adhesive bonding and product produced. 1978,
755   53.   Kinloch A J, Welch L S, Bishop H E. The Locus of Environmental Crack Growth in Bonded
756   Aluminium Alloy Joints. The Journal of Adhesion, 1984, 16(3): 165-177
757   54.   Visser P, Terryn H, Mol J M. Aerospace Coatings. In: Hughes A E, Mol J M C, Zheludkevich
758   M L, Buchheit R G, (eds). Active Protective Coatings: Springer, 2016, 315-372
759   55.   Sulka G D, Parkoła K G. Temperature influence on well-ordered nanopore structures grown by
760   anodization of aluminium in sulphuric acid. Electrochimica Acta, 2007, 52(5): 1880-1888
761   56.   Arrowsmith D J, Clifford A W. Morphology of anodic oxide for adhesive bonding of
762   aluminum. International Journal of Adhesion and Adhesives, 1983, 3(4): 193-196
763   57.   Kock E, Muss V, Matz C, De wit F. Verfahren zur anodischen oxidation. 1993, EP0607579
764   A1(
765   58.   Abrahami S T, Hauffman T, de Kok J M M, Mol J M C, Terryn H. XPS Analysis of the
766   Surface Chemistry and Interfacial Bonding of Barrier-Type Cr(VI)-Free Anodic Oxides. The Journal of
767   Physical Chemistry C, 2015, 119(34): 19967-19975
768   59.   Abrahami S T, de Kok J M M, Gudla V C, Ambat R, Terryn H, Mol J M C. Interface Strength
769   and Degradation of Adhesively Bonded Porous Aluminum Oxides npj Materials Degradation, 2017, accepted
770   60.   Kape J M. Electroplating Met. Finish., 1961, 11: 407-415

22

771   61.   Curioni M, Skeldon P, Koroleva E, Thompson G E, Ferguson J. Role of Tartaric Acid on the
772   Anodizing and Corrosion Behavior of AA 2024 T3 Aluminum Alloy. Journal of the Electrochemical Society,
773   2009, 156(4): C147-C153
774   62.   García-Rubio M, de Lara M P, Ocón P, Diekhoff S, Beneke M, Lavía A, García I. Effect of
775   postreatment on the corrosion behaviour of tartaric–sulphuric anodic films. Electrochimica Acta, 2009, 54(21):
776   4789-4800
777   63.   García-Rubio M, Ocón P, Climent-Font A, Smith R W, Curioni M, Thompson G E, Skeldon P,
778   Lavía A, García I. Influence of molybdate species on the tartaric acid/sulphuric acid anodic films grown on
779   AA2024 T3 aerospace alloy. Corrosion Science, 2009, 51(9): 2034-2042
780   64.   Kock E. Design of a novel anodic film to meet the requirements of aircraft applications. In:
781   *Proceedings of*   2004, Bremen, Germany
782   65.   van Put M, Abrahami S T, Elisseeva O, de Kok J M M, Mol J M C, Terryn H.
783   Potentiodynamic anodizing of aluminum alloys in Cr(VI)-free electrolytes. Surface and Interface Analysis,
784   2016, 48(8): 946-952
785   66.   Boeing. Process Spec. Boric Acid -- Sulfuric Acid Anodizing, Revision D. 2004, BAC 5632(
786   67.   Domingues L, Fernandes J C S, Da Cunha Belo M, Ferreira M G S, Guerra-Rosa L. Anodising
787   of Al 2024-T3 in a modified sulphuric acid/boric acid bath for aeronautical applications. Corrosion Science,
788   2003, 45(1): 149-160
789   68.   Zhang J-s, Zhao X-h, Zuo Y, Xiong J-p. The bonding strength and corrosion resistance of
790   aluminum alloy by anodizing treatment in a phosphoric acid modified boric acid/sulfuric acid bath. Surface
791   and Coatings Technology, 2008, 202(14): 3149-3156
792   69.   Yendall K A, Critchlow G W. Novel methods, incorporating pre- and post-anodising steps, for
793   the replacement of the Bengough–Stuart chromic acid anodising process in structural bonding applications.
794   International Journal of Adhesion and Adhesives, 2009, 29(5): 503-508
795   70.   Bjørgum A, Lapique F, Walmsley J. AC anodising as pre-treatment prior to adhesive bonding
796   of aluminium. 2004,
797   71.   Critchlow G W, Yendall K A, Lu J. Friendlier Surface Treatments – For Metals. Society for
798   Adhesion and Adhesives in conjunction with BASA, 2007,
799   72.   Critchlow G, Ashcroft I, Cartwright T, Bahrani D. Anodising aluminum alloy. 2011,
800   73.   Arrowsmith D J, Clifford A W. A new pretreatment for the adhesive bonding of aluminium.
801   International Journal of Adhesion and Adhesives, 1985, 5(1): 40-42
802   74.   Digby R P, Packham D E. Pretreatment of aluminium: topography, surface chemistry and
803   adhesive bond durability. International Journal of Adhesion and Adhesives, 1995, 15(2): 61-71
804   75.   Chung C K, Liao M W, Chang H C, Lee C T. Effects of temperature and voltage mode on
805   nanoporous anodic aluminum oxide films by one-step anodization. Thin Solid Films, 2011, 520(5): 1554-1558
806   76.   Underhill P R, Rider A N. Hydrated oxide film growth on aluminium alloys immersed in warm
807   water. Surface and Coatings Technology, 2005, 192(2–3): 199-207
808   77.   Rider A N. The influence of porosity and morphology of hydrated oxide films on
809   epoxy-aluminium bond durability. Journal of Adhesion Science and Technology, 2001, 15(4): 395-422
810   78.   Özkanat Ö, Salgin B, Rohwerder M, Mol J M C, de Wit J H W, Terryn H. Scanning Kelvin
811   Probe Study of (Oxyhydr)oxide Surface of Aluminum Alloy. The Journal of Physical Chemistry C, 2011,
812   116(2): 1805-1811
813   79.   Özkanat Ö, de Wit F M, de Wit J H W, Terryn H, Mol J M C. Influence of pretreatments and
814   aging on the adhesion performance of epoxy-coated aluminum. Surface and Coatings Technology, 2013,
815   215(0): 260-265

23

816   80.   Rider A N, Arnott D R. Boiling water and silane pre-treatment of aluminium alloys for durable
817   adhesive bonding. International Journal of Adhesion and Adhesives, 2000, 20(3): 209-220
818   81.   Din R U, Piotrowska K, Gudla V C, Jellesen M S, Ambat R. Steam assisted oxide growth on
819   aluminium alloys using oxidative chemistries: Part I Microstructural investigation. Applied Surface Science,
820   2015, 355: 820-831
821   82.   Din R U, Jellesen M S, Ambat R. Steam assisted oxide growth on aluminium alloys using
822   oxidative chemistries: Part II corrosion performance. Applied Surface Science, 2015, 355: 716-725
823   83.   Din R U, Jellesen M S, Ambat R. Role of acidic chemistries in steam treatment of aluminium
824   alloys. Corrosion Science, 2015, 99: 258-271
825   84.   Keller F, Hunter M S, Robinson D L. Structural Features of Oxide Coatings on Aluminum.
826   Journal of the Electrochemical Society, 1953, 100(9): 411-419
827   85.   Sulka G D. Highly Ordered Anodic Porous Alumina Formation by Self-Organized Anodizing.
828   Nanostructured Materials in Electrochemistry: Wiley-VCH Verlag GmbH & Co. KGaA, 2008, 1-116
829   86.   Parkhutik V P. The initial stages of aluminium porous anodization studied by Auger electron
830   spectroscopy. Corrosion Science, 1986, 26(4): 295-310
831   87.   Xu Y, Thompson G E, Wood G C, Bethune B. Anion incorporation and migration during
832   barrier film formation on aluminium. Corrosion Science, 1987, 27(1): 83-102
833   88.   González-Rovira L, López-Haro M, Hungría A B, El Amrani K, Sánchez-Amaya J M, Calvino
834   J J, Botana F J. Direct sub-nanometer scale electron microscopy analysis of anion incorporation to self-ordered
835   anodic alumina layers. Corrosion Science, 2010, 52(11): 3763-3773
836   89.   Ono S, Ichinose H, Masuko N. The high resolution observation of porous anodic films formed
837   on aluminum in phosphoric acid solution. Corrosion Science, 1992, 33(6): 841-850
838   90.   Thompson G E, Wood G C. 5 - Anodic Films on Aluminium. In: J.C S, (ed). Treatise on
839   Materials Science and Technology: Elsevier, 1983, 205-329
840   91.   Alexander M R, Thompson G E, Beamson G. Characterization of the oxide/hydroxide surface
841   of aluminium using x-ray photoelectron spectroscopy: a procedure for curve fitting the O 1s core level.
842   Surface and Interface Analysis, 2000, 29(7): 468-477
843   92.   van den Brand J, Blajiev O, Beentjes P C J, Terryn H, de Wit J H W. Interaction of Anhydride
844   and Carboxylic Acid Compounds with Aluminum Oxide Surfaces Studied Using Infrared Reflection
845   Absorption Spectroscopy. Langmuir, 2004, 20(15): 6308-6317
846   93.   Abrahami S T, Hauffman T, de Kok J M M, Mol J M C, Terryn H. Effect of Anodic
847   Aluminum Oxide Chemistry on Adhesive Bonding of Epoxy. The Journal of Physical Chemistry C, 2016,
848   Accepted for publication
849   94.   Wood G C, O'Sullivan J P. The anodizing of aluminium in sulphate solutions. Electrochimica
850   Acta, 1970, 15(12): 1865-1876
851   95.   Patermarakis G, Moussoutzanis K. Transformation of porous structure of anodic alumina films
852   formed during galvanostatic anodising of aluminium. Journal of Electroanalytical Chemistry, 2011, 659(2):
853   176-190
854   96.   Thompson G E. Porous anodic alumina: fabrication, characterization and applications. Thin
855   Solid Films, 1997, 297(1–2): 192-201
856   97.   Curioni M, Skeldon P, Thompson G E. Anodizing of Aluminum under Nonsteady Conditions.
857   Journal of the Electrochemical Society, 2009, 156(12): C407-C413
858   98.   Han X Y, Shen W Z. Improved two-step anodization technique for ordered porous anodic
859   aluminum membranes. Journal of Electroanalytical Chemistry, 2011, 655(1): 56-64

24

860 99.   Aerts T, Dimogerontakis T, De Graeve I, Fransaer J, Terryn H. Influence of the anodizing
861 temperature on the porosity and the mechanical properties of the porous anodic oxide film. Surface and
862 Coatings Technology, 2007, 201(16–17): 7310-7317
863 100.   Stępniowski W J, Bojar Z. Synthesis of anodic aluminum oxide (AAO) at relatively high
864 temperatures. Study of the influence of anodization conditions on the alumina structural features. Surface and
865 Coatings Technology, 2011, 206(2-3): 265-272
866 101.   Aerts T, Jorcin J-B, De Graeve I, Terryn H. Comparison between the influence of applied
867 electrode and electrolyte temperatures on porous anodizing of aluminium. Electrochimica Acta, 2010, 55(12):
868 3957-3965
869 102.   Schneider M, Kremmer K, Weidmann S K, Fürbeth W. Interplay between parameter variation
870 and oxide structure of a modified PAA process. Surface and Interface Analysis, 2013, 45(10): 1503-1509
871 103.   Terryn H. Electrochemical investigation of AC electrograining of aluminium and its porous
872 anodic oxidation. Brussel: Vrije Universiteit Brussel, 1987
873 104.   Zaraska L, Sulka G D, Szeremeta J, Jaskuła M. Porous anodic alumina formed by anodization
874 of aluminum alloy (AA1050) and high purity aluminum. Electrochimica Acta, 2010, 55(14): 4377-4386
875 105.   Curioni M, Scenini F. The Mechanism of Hydrogen Evolution During Anodic Polarization of
876 Aluminium. Electrochimica Acta, 2015, 180: 712-721
877 106.   Curioni M, Saenz de Miera M, Skeldon P, Thompson G E, Ferguson J. Macroscopic and
878 Local Filming Behavior of AA2024 T3 Aluminum Alloy during Anodizing in Sulfuric Acid Electrolyte.
879 Journal of the Electrochemical Society, 2008, 155(8): C387-C395
880 107.   Schneider M, Yezerska O, Lohrengel M M. Anodic oxide formation on AA2024:
881 electrochemical and microstructure investigation. Corrosion Engineering, Science and Technology, 2008,
882 43(4): 304-312
883 108.   Saenz de Miera M, Curioni M, Skeldon P, Thompson G E. The behaviour of second phase
884 particles during anodizing of aluminium alloys. Corrosion Science, 2010, 52(7): 2489-2497
885 109.   Garcia-Vergara S J, El Khazmi K, Skeldon P, Thompson G E. Influence of copper on the
886 morphology of porous anodic alumina. Corrosion Science, 2006, 48(10): 2937-2946
887 110.   Kollek H. Some aspects of chemistry in adhesion on anodized aluminium. International
888 Journal of Adhesion and Adhesives, 1985, 5(2): 75-80
889 111.   Packham D E. Surface energy, surface topography and adhesion. International Journal of
890 Adhesion and Adhesives, 2003, 23(6): 437-448
891 112.   Packham D E, Johnston C. Mechanical adhesion: were McBain and Hopkins right? An
892 empirical study. International Journal of Adhesion and Adhesives, 1994, 14(2): 131-135
893 113.   Allen K W. Some reflections on contemporary views of theories of adhesion. International
894 Journal of Adhesion and Adhesives, 1993, 13(2): 67-72
895 114.   van den Brand J, Blajiev O, Beentjes P C J, Terryn H, de Wit J H W. Interaction of Ester
896 Functional Groups with Aluminum Oxide Surfaces Studied Using Infrared Reflection Absorption
897 Spectroscopy. Langmuir, 2004, 20(15): 6318-6326
898 115.   Özkanat Ö, Salgin B, Rohwerder M, Wit J, Mol J, Terryn H. Interactions at
899 polymer/(oxyhydr) oxide/aluminium interfaces studied by Scanning Kelvin Probe. Surface and Interface
900 Analysis, 2012, 44(8): 1059-1062
901 116.   Abrahami S T, Hauffman T, de Kok J M M, Mol J M C, Terryn H. Effect of Anodic
902 Aluminum Oxide Chemistry on Adhesive Bonding of Epoxy. The Journal of Physical Chemistry C, 2016,
903 120(35): 19670-19677

25

904   117.   Abrahami S T, Hauffman T, de Kok J M M, Terryn H, Mol J M C. The role of acid-base

905   properties in the interactions across the oxide-primer interface in aerospace applications. Surface and Interface

906   Analysis, 2016, 48(8): 712-720

907

1   Front. Chem. Sci. Eng.

3   REVIEW ARTICLE

4   Towards Cr(VI)-free Anodization of Aluminum Alloys for

5   Aerospace Adhesive Bonding Applications: A Review

6   Shoshan T. ABRAHAMI [1,2], John M.M. DE KOK [3], Herman TERRYN [2,4], Johannes M.C. MOL (□) [2]

7   1 *Materials innovation institute (M2i), Elektronicaweg 25, 2628 XG, Delft, The Netherlands*

8   2 *Delft University of Technology, Department of Materials Science and Engineering, Mekelweg 2, 2628*
9   *CD, Delft, The Netherlands*

10 3 *Fokker Aerostructures BV, Industrieweg 4, 3351 LB, Papendrecht, The Netherlands*

11 4 *Department of Materials and Chemistry, Research Group Electrochemical and Surface Engineering*
12 *(SURF), Vrije Universiteit Brussel, Pleinlaan 2, 1050 Brussels, Belgium*

16 **Abstract**

17 For more than six decades, chromic acid anodizing (CAA) has been the central process in the surface
18 pre-treatment of aluminum for adhesively bonded aircraft structures. Unfortunately, this electrolyte
19 contains hexavalent chromium (Cr(VI)), a compound known for its toxicity and carcinogenic properties.
20 To comply with the new strict international regulations, the Cr(VI)-era will soon have to come to an end.
21 Anodizing aluminum in acid electrolytes produces a self-ordered porous oxide layer. Although different
22 acids can be used to create this type of structure, the excellent adhesion and corrosion resistance that is
23 currently achieved by the complete Cr(VI)-based process is not easily matched. This paper provides a
24 critical overview and appraisal of proposed alternatives to CAA, including combinations of multiple
25 anodizing steps, pre- and post anodizing treatments. The work is presented in terms of the modifications
26 to the oxide properties, such as morphological features (e.g. pore size, barrier layer thickness) and surface
27 chemistry, in order to evaluate the link between fundamental principles of adhesion and bond
28 performance.

31

1 Introduction

For many years, hexavalent chromium has been used for the corrosion protection of metals in many industries; aerospace, automotive, maritime and architectural structures are just a few examples for the wide spectrum of applications in which Cr(VI)-based coatings can guarantee the life-long integrity of metallic parts. Unfortunately, Cr(VI) is regarded to be extremely toxic and carcinogenic [1, 2]. This has already being noticed in the first decades of the 20th century [3, 4]. Numerous studies have shown that employees working with chromate-containing compounds risk exposure through skin contact and by inhalation of vapors or dust particles [5, 6]. In the aerospace industry this mostly occurs in the production stage, when the parts are pretreated and painted, during their maintenance or at the end-of life, when these coatings and paints are removed.

In 2006, the Occupational Safety and Health Administration (OSHA) in the U.S. [7], the European Registration, Evaluation, Authorization and Restriction of Chemicals (REACH, EC n°1907/2006) and Restriction of Hazardous Substancespolicies (RoHS) introduced new regulations that strictly limit the use of hexavalent chromium and announced its near future ban. As a consequence, chromates are no longer used in most commercial processes and products. However, the corrosion sensitivity of high-strength aluminum alloys and the required level of performance and safety make its overall replacement in the aerospace industry a very challenging task. In addition, the time it takes to test and qualify new systems for aviation is much longer compared to that in other industries. Therefore, Cr(VI)-based substances are currently still utilized in most aerospace metal pre-treatment, coating and bonding processes.

This paper reviews the state-of-the-art alternatives to *chromic acid anodizing* (CAA), which is the key pre-treatment step to produce anodic oxide films suitable for adhesive bonding. Herein, only the manufacturing of parts aimed for *structural* components are discussed. Although other components of the aircraft are produced in a similar manner, structural components are considered the most critical since they are designed as part of the principal load-carrying structure of the aircraft and they are typically not accessible for inspection and maintenance during its lifetime [8]. As such, these components are subject to the highest engineering standards.

The following section provides background on the main issues and challenges in the pre-treatments of aluminum for structural bonding. Next, section three presents the development of the benchmark CAA process that is currently used in Europe and its major oxide characteristics. The fourth section covers the range of Cr(VI)-free alternatives. In order to identify the key factors that determine the adhesion and durability of these structures, section five critically reviews the main processing parameters, as concluded by reviewing the literature available to date, including recent detailed investigations by the authors. The final section discusses the relation between the main oxide properties and bond performance. This review paper ends with a short summary and conclusion in section six.

2. Structural adhesive bonding in aircraft structures

Adhesive bonding is one of the oldest techniques to join different components, often of dissimilar nature [9]. Bonding is established when the adhesives undergoes physical or chemical hardening reaction (curing) to join the two panels together through surface adherence (adhesion) and internal strength (cohesion) [10]. Adhesive bonding was already used in the first aircrafts, which were made from wood

2

71   and continued in the 1940s, when manufacturers started using aluminum [11]. Since then adhesive
72   bonding has become a standard technique to produce the main body (fuselage), wings and other parts of
73   modern aircrafts [12]. Fig. 1 shows the main steps in the production of adhesively bonded components at
74   *Fokker Aerostructures* in the Netherlands.

75   **Figure 1** The production of metal-to-metal bonding at Fokker Aerostructures: (a) surface pre-treatment (panels hanging
76   above the anodizing bath), (b) parts drying on the rack after pre-treatment, (c) primer application, (d) adhesive application,
77   (e) a bonded part.

2.1 Durability of the adhesive bond

79   Ideally, the bonded structure will be able to withstand and carry the high loads that are executed on the
80   structure during use and efficiently transfer and distribute the mechanical stresses over a large surface
81   area. A crucial parameter in maintaining the long-term integrity of the assembly is durability of adhesion
82   under various environmental conditions, such as temperature extremes, varying atmospheric pressures,
83   moisture content and types of aggressive species (e.g. anti-freeze and chlorine ions). These, in
84   combination with the varying mechanical stresses, may lead to early failure [13]. Fig. 2 illustrates the
85   different possible failure mechanisms that can occur within an adhesive joint. They are generally
86   characterized as predominantly cohesive- or adhesive in nature. Cohesive failures take place within the
87   same phase, whereas adhesive failures occur at their interfaces.
88   Industrial standards generally demand higher adhesion than cohesion strengths. This is desired from an
89   engineering point of view, since cohesive failure related to bulk material properties could be readily
90   considered by design. In the case of metal-to-metal adhesive bonding, this refers to a cohesive failure
91   within the polymeric adhesive (Fig. 2 (A)). Other failure mechanisms (Fig. 2 (B)-(F)) are usually the
92   result of poor bond preparation (processing) and effects of environmental conditions.
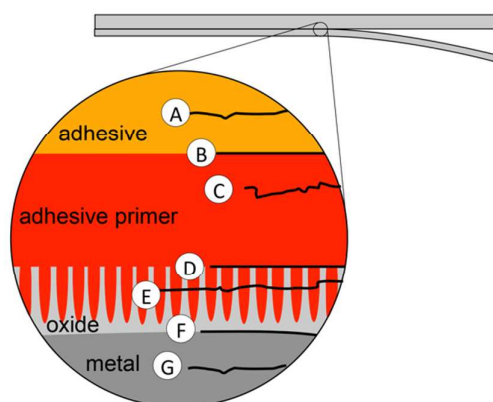
3

93

94   **Figure 2** Schematic illustration of the possible failure modes in structural adhesive joint: (A) cohesive fracture of the
95   adhesive film, (B) interfacial disbonding between adhesive and primer, (C) cohesive fracture of primer layer, (D)
96   interfacial disbonding between primer and anodic coating, (E) fracture within anodic oxide coating and (F) corrosion of
97   aluminum substrate at metal/oxide interface and (G) failure of the metal substrate.

98

99   One of the key issues concerning bond durability is the permeability of water molecules. Moisture from
100 the environment can enter the bonded system by bulk diffusion through the adhesive, by interfacial
101 diffusion along the interface between the adhesive and the oxide, and by capillary action through cracks
102 or defects. Zanni-Deffarges and Shanahan [14] compared diffusion rates in bulk and bonded epoxy
103 adhesive to show that capillary effects near the oxide-polymer interface can significantly enhance the
104 diffusion rate of water in bonded joints. Once reaching the bond line, moisture can hydrate the oxide.
105 This leads to the formation of oxyhydroxides, a weaker form of oxide with a larger volume [15].
106 Ultimately, this can lead to cohesive fracture within the hydrated oxide (Fig. 2 (E)). Alternatively, the
107 presence of water at the interface can displace the previously formed bonds between the oxide and the
108 resin, leading to delamination by de-adhesion (Fig. 2 (D)). Another dangerous failure mode is *bondline*
109 *corrosion* (Fig. 2 (F)). It occurs when a relatively pure aluminum clad layer is present, which function as
110 a sacrificial anode to the base materials. Also this type of failure is facilitated by the diffusion of water
111 and other corrosion-initiating species (e.g. chlorine ions). Once bondline corrosion is initiated, it is
112 characterized by disbonding at the interface followed by localized corrosion.
113 Pure aluminum metal has an inherent corrosion resistance due to the presence of a relatively uniform and
114 thin oxide layer that protects the underlying metal [16]. This is caused by the high affinity of aluminum
115 towards oxygen. Whenever the fresh metal surface is exposed to the atmosphere as, for example, in case
116 of mechanical damage a new oxide layer will be formed. In dry conditions, this oxide film is typically a
117 dense barrier layer of amorphous alumina (Al_2O_3) that is only 2 to 3 nm thick. In humid environments,
118 this oxide will be covered by a more permeable hydrated aluminum hydroxide ($Al_2O_3 \cdot xH_2O$) at the outer
119 surface. In that case the thickness of this layer can reach up to 10 nm [16]. These thin oxide layers are
120 stable over a fairly broad range of pH ($4 < pH < 8.5$), providing aluminum with sufficient protection for
121 various commercial purposes. At both lower and higher pH values this layer is not stable and it will
122 dissolve [17].
123 Nevertheless, aluminum in aerospace applications is mainly used in its alloy form. The most commonly
124 employed types of aluminum in the aerospace industry belong to the 2xxx and 7xxx alloy series. Within
125 these families, AA2024-T3 and AA7075-T6 are the most used ones to date. The main alloying elements
126 include copper (Cu), magnesium (Mg) and manganese (Mn) in AA2024 and zinc (Zn), magnesium (Mg),

4

127 copper (Cu) and silicon (Si) in AA7075. [18]. These heat-treatable alloys develop their strength by
128 precipitation hardening. As a consequence, the microstructure of these alloys is very complex, presenting
129 several second phase and intermetallic particles. The addition of alloying elements, though essential for
130 mechanical properties, can have detrimental consequences on to the substrate's corrosion resistance. The
131 electro potential differences between local areas of compositional differences can lead to galvanic
132 coupling and selective dissolution of the more active element. The most common type of corrosion in
133 aluminum alloys is pitting corrosion due to second phase particles in the matrix acting as cathodes or
134 grain boundary precipitation causing precipitate-free zones. These phenomena are especially pronounced
135 in AA2024-T3, which contains relatively high amounts of copper, a nobler element to aluminum. These
136 localized attacks can proceed to considerable depths within the substrate and may lead to grain fallout
137 when proceeding along grain boundaries. Detailed mechanisms of localized corrosion of AA2024-T3
138 under chloride conditions can be found elsewhere in the literature [19-21].

139 Additionally to their corrosion sensitivity, the surface of the substrate in its 'as-received' state is not
140 suitable for bonding. Metallurgical processing, including heat treatment and rolling, modifies the
141 uppermost layers of the alloy surface. Fig. 3 presents a schematic illustration of these layers, which
142 displays both compositional and structural changes, including smaller grains, enrichments in secondary
143 particles (dispersoids) and higher concentration of Mg and Zn [22]. Additionally, the high shear forces
144 applied during rolling are able to break and fold some of the surface oxides into the substrate. Altogether,
145 this result in a so-called 'near-surface deformed layers' (NSDL), which present significant different
146 electrochemical and mechanical properties compared to the bulk material. [23]. Hence, removing these
147 NSDL should be the first step in any type of further processing.

148 **Figure 3** Schematic illustration of the modified composition of the aluminum alloy surface present after metallurgical
149 processing [22].

150

3. Chromic acid anodizing (CAA)

152 In order to avoid the previously mentioned types of failure and to ensure long-term safety, bonded
153 metal-to-metal assemblies must be carefully prepared. Surface pre-treatment has emerged as the most
154 important step to provide the desired surface characteristics for bonding and minimize the effect of

5

155 surface heterogeneities, as the NSDL. The main pre-treatment schedule that is currently applied in the
156 aerospace industry is illustrated in Fig. 4. It consists of four major steps: degreasing, pickling (or
157 etching), anodizing, and primer application, all currently relying on Cr(VI)-based chemicals. In between
158 two subsequent steps the surface is thoroughly rinsed in water. The following subsections describe each
159 step of this pre-treatment scheme in terms of how it modifies the surface properties and its historical
160 context.

| As received Al alloy | Degreasing incl. $Na_2Cr_2O_7$ | Pickling with acids + CrO_3/ $Na_2Cr_2O_7$ | Chromic acid anodizing (CAA) | Primer with $SrCrO_4$ |

Processing time →

161 **Figure 4** schematic representations of the process steps and the modifications that take place during the complete Cr-based
162 pre-treatment that is currently applied in the European aerospace industry.

163

164 **Degreasing** is the first step in the pre-treatment process and normally the minimum preparation that is
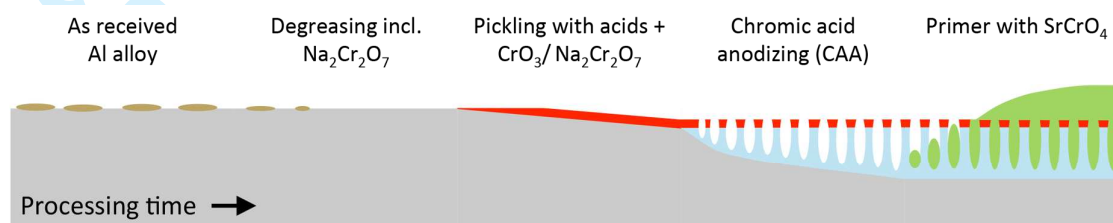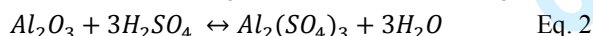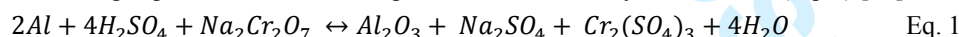165 carried out prior to any type of metal bonding. Degreasing removes any oils, grease and contaminations
166 that might have been introduced during aluminum manufacturing and processing [24]. This preliminary
167 cleaning is necessary to assure that the following steps will work evenly across the substrate surface [16].
168 Next, the modified surface layers are chemically removed by **pickling** (also called etching). This can be
169 performed in either acidic or alkaline solutions. The classical pickling solutions are often composed from
170 mixtures of chromic and sulfuric acids and they are generally divided into two types: the FPL- and the
171 CSA etch [25]. The first is the *Forest Products Laboratory* (FPL) process that was developed in the
172 1950s in the U.S. It consists of immersing the substrate in sodium dichromate ($Na_2Cr_2O_7$) and sulfuric
173 acid solution for 9-15 min at 65°C. The European version of this etch, the CSA pickling, uses lower
174 concentrations of either chromium trioxide (CrO_3) or sodium dichromate ($Na_2Cr_2O_7$) with sulfuric acid at
175 similar temperatures, but longer immersion times (30 min.) [26]. Both methods follow a two-step
176 reaction mechanism. In the first step, hexavalent chromium catalyses the oxidation of aluminum to
177 alumina following Eq. 1. Next, the alumina product is dissolved by sulfuric acid (Eq. 2) [16].

178 $$2Al + 4H_2SO_4 + Na_2Cr_2O_7 \leftrightarrow Al_2O_3 + Na_2SO_4 + Cr_2(SO_4)_3 + 4H_2O \qquad \text{Eq. 1}$$
179 $$Al_2O_3 + 3H_2SO_4 \leftrightarrow Al_2(SO_4)_3 + 3H_2O \qquad \text{Eq. 2}$$

180 Since the second step is slower than the first one, a thin oxide layer is produced on the surface (as
181 indicated by the red layer in Fig. 4). This oxide is amorphous, with a composition corresponding to
182 alumina (Al_2O_3) and some minor concentrations (~0.5%) of Cr and S impurities. Venables et al. [27]
183 reported that due to surface energy interactions, whiskers-like protrusions extending from the triple grain
184 boundary points extend up to 40 nm from the surface. In their paper, the authors suggest that these
185 branched protrusions already provide sufficient interlocking with the adhesive surface, resulting in an
186 improved adhesion.
187 Unfortunately, some early in-service failures (mostly of non-bonded structures) occurred in the
188 beginning of the 1960s, as aircrafts manufacturers started using epoxy adhesives instead of phenols [26].
189 The relatively thin oxide film was thus insufficient to provide reproducible and durable bonds.
190 Consequently, an extra step, anodizing, was added to the pre-treatment schedule. **Anodizing** is an
191 electrochemical process in which the aluminum substrate is artificially oxidized to grow a thick oxide
192 film (up to several μm) [16]. The process derives its name from the fact that the aluminum substrate is

6

193 used as the anode in an electrolytic cell. The anode (substrate) is connected to the positive terminal of a
194 DC power supply while a cathode (e.g. Al, stainless steel) is connected to the negative terminal. When
195 the circuit is closed, electrons are withdrawn from the aluminum anode, which facilitate the oxidation of
196 aluminum atoms to aluminum cations (Al^{3+}) at the metal/oxide interface. This is illustrated in Fig. 5.
197 Since the electronic conductivity of aluminum oxide is very low, the anodizing voltage that is applied on
198 the anodic cell encounters a resistance by the existing (natural) oxide film. This leads to a potential drop
199 over the metal/electrolyte interface, which give rise to high electric field over the oxide layer. These
200 electric fields are typically in the order of 10^6 to 10^7 V/m [28], which is high enough to enable oxide
201 growth by ionic migration through the oxide [29]. Since aluminum is anodized in an aqueous electrolyte,
202 adsorbed water at the anode will break down forming negatively charged O^{2-} and OH^-. These anions
203 migrate towards the positively charged anodic substrate. A reaction between Al^{3+} and O^{2-} will leads to
204 the formation of alumina, Al_2O_3, at the metal/oxide interface. Since not all the produced Al^{3+} is
205 consumed by this interface, excess Al^{3+} cations will migrate away from the positively charged anode.
206 Upon reaching the oxide/electrolyte interface, Al^{3+} can react with available O^{2-} forming additional
207 alumina at the oxide/electrolyte interface. Under certain conditions, alumina ions will be directly ejected
208 into the electrolyte. The conversion efficiency and, hence, final film morphology will depend on the
209 balance between oxide growth and oxide dissolution (through direct ejection and chemical attack by an
210 aggressive electrolyte). This in turn, is determined by the nature of the electrolyte and the process
211 conditions, as discussed later.

212
213
214
215
216
217
218
219
220

221 **Figure 5** Schematic representation of the aluminum/electrolyte interface, showing the ionic processes involved in oxide
222 growth during anodizing [30].

223 Chromic acid anodizing (CAA) was incorporated into the pre-treatment schedule in the 1960s. It mainly
224 aimed to improve the overall corrosion resistance by producing a thicker physical barrier between the
225 metal and its environment. Although anodizing can produce barrier- and porous-type oxide
226 morphologies, porous films are preferred for bonding purposes. As illustrated in Fig. 6, porous anodic
227 oxides consist of a compact barrier layer on the bottom and a relatively regular hexagonal porous
228 structure on top [31-34]. These films are created when the anodic oxide is sparingly soluble in the
229 anodizing electrolyte [31, 35]. In Europe, the 40/50V Bengough-Stuart process was adapted, using
230 2.5-3.0 wt.% chromic acid (CrO_3) at 40 °C [36]. The voltage across the electrolytic bath is initially raised
231 to 40V in the first 10 minutes. This voltage is then maintained for 20 more minutes before it is raised to
232 50V, where it is kept constant during the last 5 minutes [37]. The higher voltage at the end results in a
233 thicker barrier layer, providing an extra thick barrier for corrosive species [38].
234

235   **Figure 6** An idealized illustration of the anodic oxide structure formed on clad alloys following the 40/50 V CAA process

236   [36].

237

238   This process produces 3-4 μm thick oxide layers on both AA2024-T3 and AA7075-T6 (bare and clad). It

239   is a relatively ductile oxide with very low (0.1-0.3 wt.%) chromium content in the oxide. The oxide is
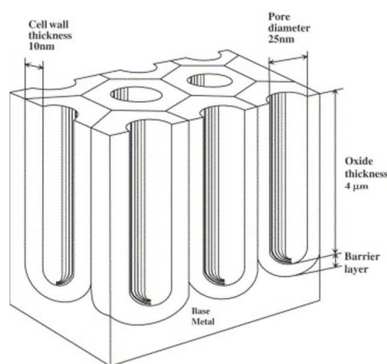
240   moderately resistant to attack by moisture, although hydration has been reported [24]. This treatment,

241   combined with prior CSA etching, was soon established as an effective pre-treatment for adhesive

242   bonding and become an industrial standard.

243   In regular manufacturing operations, a certain time interval (several hours up to several months) usually

244   passes between substrate pre-treatment and bonding. During this time, the freshly prepared oxide is

245   susceptible to damage, contaminations, and environmental degradation [39]. This is prevented by the

246   application of a thin layer of **primer** to seal the oxide immediately (within two hours) after the

247   pre-treatments, when surface activity is maximal. Primers are diluted polymeric coatings, usually

248   matching the chemistry of the adhesive. The primer functions as a physical barrier between the pretreated

249   surface and its surrounding. Except for surface protection, primers are also used to promote adhesion.

250   Two contributing mechanisms can be distinguished; (1) improved surface wetting and (2) providing

251   stronger chemical interactions. The first mechanism is driven by the primer's lower viscosity (compared

252   to the adhesive) and the addition of wetting agents. Kinloch et al, [40] compared PAA films that were

253   bonded with- and without primer to show that a primer is able to penetrate deep and completely fill the

254   pores, providing better adhesion. The second mechanism uses coupling agents to form a covalent bond

255   across the inorganic-organic interface. Coupling agents are molecules with dual functionality. They

256   contain organic end- groups such as methoxy (CH_3O-), ethoxy (CH_3CH_2O-) or hydroxyl (HO-) attached

257   to a metallic central atom (e.g. silicon, zirconium or titanium) [41]. Organosilane coupling agents are the

258   predominant chemical type of adhesion promoters. These groups are able to adsorb on the metal oxide

259   surface through hydrogen bonds. Upon curing, a metallosiloxane bonds (Al-O-Si) are formed with the

260   surface oxide [42]. These covalent bonds are much stronger than hydrogen bonds. Any remaining silanol

261   groups will condense with themselves, forming a dense Si-O-Si network. Since Al-O-Si bond can be

262   hydrolysed, the durability of these bonds will be determined by the extent of cross-linking of the Si-O-Si

263   bonds, which will determine the hydrophobicity of the covering siloxane film. Hence, adjusting the

264   chemical composition to tailor the desired film properties is essential. It is important to also match the

265   reactivity of the coupling agent with that of the adhesive [41]. Different studies have demonstrated that

266   silanes are capable to improve interfacial adhesion [40, 43-45], as well as corrosion resistance of coated

267   aluminum [46, 47]. Song and van Ooij [48], for example, have shown that by combining two types of

268   silanes, namely 1,2-bis(triethoxysilyl)ethane (BTSE) and ϒ-aminopropyltriethoxy (ϒ-APS), it is possible

8

269 to design a dual functionality interface that would give good corrosion protection and will be compatible
270 with an epoxy adhesive. Since silanes connect via the OH- groups on the substrate, maximizing their
271 amount on the substrate is desired. A study by Franquet et al. [49], showed that chemical pre-treatments
272 affecting the amount of surface hydroxyl groups will in turn affect the silane film uniformity and
273 thickness. Therefore, when silanes are applied, prior surface pre-treatment is still needed.

274 4. Cr(VI)-free alternatives to CAA

275 Health and environmental issues, together with the increasing costs associated with the treatment and
276 disposal of solutions containing hexavalent chromium initiated a large number of studies over the past
277 decades. To avoid an exhaustive comparison of the different process parameters, this section will focus
278 on the different methods rather than specific outcomes of the most relevant alternative Cr(VI)-free
279 pre-treatments for structural bonding. For a detailed list of the specific pre-treatments and evaluation
280 techniques, readers are encouraged to consult the review published by Critchlow and Brewis [24].

281 4.1 Phosphoric acid anodizing (PAA)

282 For economic reasons, anodizing was initially rejected in the US until Boeing introduced phosphoric acid
283 anodizing (PAA) in 1975, which makes PAA the first commercial alternative to CAA. The PAA process
284 applies 10wt.% phosphoric acid at 21-24 °C. Anodizing is conducted at constant voltage of 10-15 V for
285 25 minutes. The PAA oxide is considerably thinner (typically 0.5 to 2 μm) and more porous than the
286 CAA film [50]. However, it has an advantage, since the composition of the outer part of the film
287 corresponds to non-hydrated $AlPO_4$ in the outer layer (see section 5.2), which provides higher resistance
288 to humidity and even to hot water sealing. This resistance is attributed to the stability of the chemical
289 bonds between aluminum and phosphate [51] [52] and, therefore, provides an effective environmental
290 stability during service [53]. Nevertheless, studies show that the corrosion resistance of PAA oxides is
291 inferior to those of CAA, which explains why this process was developed together with the introduction
292 of chromate inhibiting primers. Hence, although the PAA process is Cr(VI)-free it typically requires the
293 additional support of (active) protective coatings that contain corrosion inhibitors. So far, the most
294 effective inhibitors are Cr(VI)-based pigments and the search for Cr(VI)-free alternatives is still in
295 progress. Some green inhibitors are based on inorganic species (including lithium, Cr(III), rare-earths,
296 molybdates and vanadates), while others are base on organic functionalities [54].

297 4.2 Mixed electrolytes anodizing

298 In addition to PAA, one of the most popular anodizing electrolytes is sulfuric acid. Conversely to PAA,
299 sulfuric acid anodizing (SAA) generally produces a thick and dens protective layer [55]. Therefore, SAA
300 is commercially applied (mostly in '*hard*' conditions) for decorative and corrosion protection
301 applications. However, the same properties that provides it with excellent corrosion and wear resistance
302 deliver poor adhesion [56]. One method to overcome this limitation is to mix sulfuric acid in the
303 anodizing bath with the more aggressive phosphoric acid, thereby providing the conditions to produce an
304 intermediate oxide structure with morphological dimensions comparable to CAA. The process, named
305 phosphoric-sulfuric acid anodizing (PSA) was developed by Kock et al. [57]. The first PSA process
306 contains equal amounts of sulfuric- and phosphoric acids (100 g/l). Similar to PAA, phosphates are found
307 in the outer layer of the oxide [58], providing an additional hydration resistance. Recent investigations by
308 the authors covered a broad range of process parameters: different concentrations of phosphoric and

9

309   sulfuric acids, together with ranging temperature and duration in the search for the optimal PSA
310   conditions [59]. Oxide films with wide morphological variations (e.g. pore size of 5 to 60 nm and layer
311   thicknesses of up to 6 μm) were prepared by changing the anodizing conditions (especially phosphoric
312   acid concentration and electrolyte temperature). These conditions were found important for the
313   performance of the bond, as tested by dry and wet floating roller peel tests. Currently, the PSA process is
314   considered a viable alternative to CAA and will be implemented at Fokker Aerostructures in the near
315   future.

316   Already in the 1960s, a mixture of tartaric and sulfuric acid anodizing (TSA) was suggested by Kape
317   [60]. Unfortunately, the resulting porosity is relatively low and adhesives cannot easily permeate into the
318   oxide layer. Hence, the analogous TSA process is mainly used in *non-structural* applications. The role of
319   tartaric acid, according to a study by Curioni et al. [61] is reducing the current density and thereby
320   reducing the oxide growth rate, so that the of the final film thickness is lower than for normal SAA. More
321   interestingly, however, an improved corrosion resistance is observed. This resistance is explained by a
322   "buffering effect" that tartarate ions remnants in the oxide are providing. During anodizing, tartaric acid
323   can combine with aluminum cations to produce aluminum tartrate, a compound that is highly soluble in
324   the acidic anodizing solution but with relatively low solubility in water. During subsequent rinsing, the
325   pH is rapidly increased and relatively large amounts of aluminum tartrate may precipitate at the pore
326   walls. As a consequence, if the oxide is exposed to a corrosive environment during its use, aluminum
327   tartrate may re-dissolve, producing a local buffer, thereby limiting the susceptibility to localized
328   corrosion. Even further improvements in the corrosion resistance of TSA films were registered after hot
329   water sealing [62] and by the addition of molybdate salts into the anodizing bath [63].

330   4.3 Two-step anodizing

331   Relying on this TSA advantage, a new type of processes has emerged, which combines two-step
332   anodizing. In this case TSA anodizing follows PSA to provide a duplex oxide with both corrosion
333   resistance and adhesion capabilities. The resulting structure shown in Fig. 7 (a) is reported to be suitable
334   for adhesive bonding of structural components [64].

335

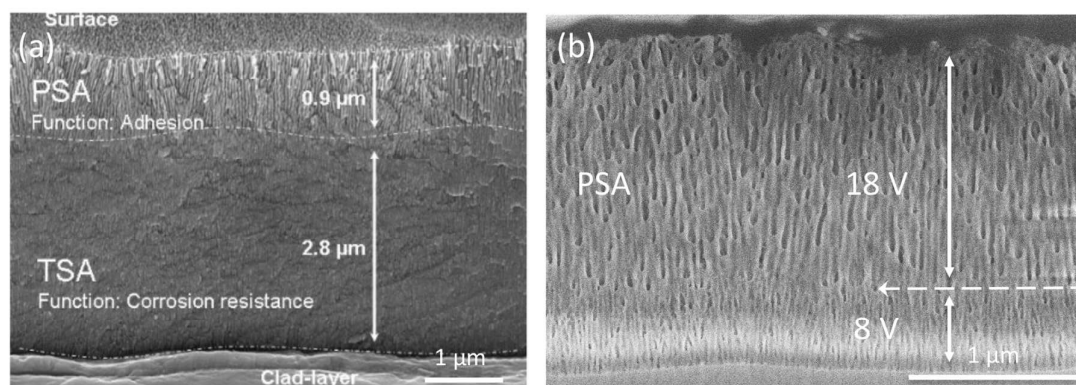336   **Figure 7** Cross section of the anodic oxide produced on 2024-T3 clad by (a) TSA+PSA process [64] and (b) PSA dynamic
337   anodizing, with voltage decrease from 18 V to 9 V [65].

338   Similar process is the boric-sulfuric acid anodizing (BSAA) that has been patented by Boeing as an
339   alternative to CAA [66]. The oxide structure resembles SAA, but with finer pores and more uniform

10

340 hexagonal arrangement compared to CAA, showing promising results [67]. Zhang et al. [68] report an
341 improvement in bonding and durability of panels created by the BSAA process by the addition of
342 phosphoric acid to the anodizing electrolyte. The process is reported to result in bigger pores, improving
343 primer penetration and extending oxide durability. Because boric acid is also hazardous, using it as a
344 replacement is not generally desired, especially since it may be subject to future regulations.

345 Similarly to two-step anodizing, dynamically changing the anodizing voltage/current during the process
346 can be used to vary the oxide morphology across its thickness. A SEM cross section of such an example
347 is shown in Fig. 7 (b), possibly providing an alternative for a two-step anodizing process. In an
348 investigation by van Put et al. [65] this complex oxide morphology was formed by an instantaneous
349 voltage decrease during anodizing. Since the pore size is linearly related to the applied voltage, an
350 instantaneous decrease from 18V to 9V forces the formation of new pores with smaller diameters below
351 existing larger pores. As a result, a distinct border between the two morphologies is formed (indicated by
352 the arrow in Fig. 7 (b)). Conversely, applying a voltage increase did not produce the reverse morphology
353 and a transition layer was formed by partly dissolving the walls of smaller pores after the sudden change.

354 ## 4.3 Electrolytic deoxidation

355 Earlier study by Venables et al. [27] have shown that fine oxide protrusions produced by the FPL etch on
356 top of a PAA oxide are beneficial for good adhesion. This is desired from adhesion point of view,
357 because protrusions, even just nanometers long, create an additional reinforcement by interlocking with
358 the resin. Likewise, Yendall and Critchlow [69] suggests a method that applies electrolytic phosphoric
359 acid deoxidizer (EPAD) before anodizing. In that respect EPAD replaces the FPL etch in producing an
360 open top layer that comes into contact with primer/adhesive (Fig. 8). They found that this method
361 improves the mechanical properties of the bond depending, however, also on the anodizing temperature
362 used for SAA. In this case, it is important to keep in mind that the choice of electrolyte and applied
363 temperature will also affect the resulting morphology. As discussed later in sections 5.1 and 5.4, if the
364 anodizing conditions are too aggressive, the EPAD layer may (in part or completely) dissolve during
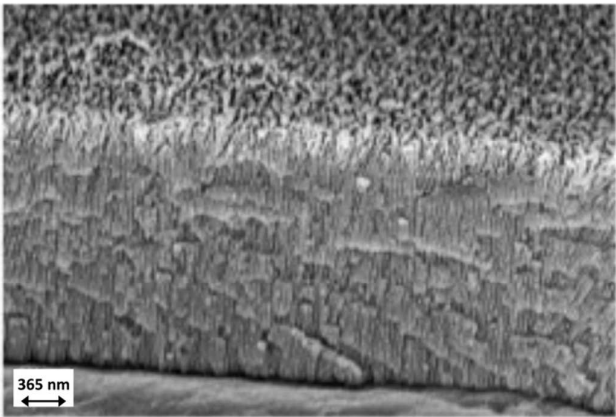365 subsequent anodizing.

366　　　　　　　　　　　**Figure 8** Cross section of AA2024-T3 clad after EPAD and SAA [69].

367 ## 4.4 AC Anodizing

11

368 An interesting alternative applies alternating current (AC) instead of the traditional direct current (DC)
369 for anodizing. AC anodizing was originally developed for high-speed coil applications in the automotive
370 industry [16]. Relatively elastic oxide layers are developed by treatment at higher temperatures and
371 higher anodizing currents. Both sulfuric- and phosphoric acid processes have been reported, with the
372 conditions listed in Table 1. Though developed as a continuous process, batch operation is also possible.

373

Table 1 Anodizing parameters [70].

Parameter	H_3PO_4	H_2SO_4
Acid concentration, wt.%	10	15
Temperature, °C	50	80
Time, min.	12	30
Current, A/dm^2	4	10

374
375
376
377
378

379 As in other AC processes, hydrogen evolves on the surface of the anode during the cathodic cycle. This
380 is sufficient to remove organic contaminants as well as natural present oxides, so that separate steps for
381 cleaning and deoxidizing prior to anodizing are not required, thereby drastically reducing the amount of
382 processing tanks [70]. Since the resulted oxides are thin, their performance is comparable to the etching
383 rather than anodic oxides [71]. Hence, a U.S. patent by Critchlow et al. [72] suggests applying a two-step
384 process that includes subsequent AC and DC PSA anodizing in the same bath. This combination
385 produces an oxide film that has a thin porous outer layer (less than 1 μm) and a relatively thick (up to 8
386 μm) uniform inner layer to yield an optimal combination of corrosion protection by the dense inner layer,
387 and adhesion provided by the porous outer layer.

388 ## 4.5 Anodizing with post-treatments

389 Correspondingly, a post-treatment immersion of the relatively dense anodic oxide in a dilute acidic or
390 alkaline solution will produce the desired morphology by chemically attacking the oxide to partly
391 dissolve it and open the pores. Both Arrowsmith and Clifford [73] and Yendall and Critchlow [69]
392 applied phosphoric acid dip after SAA (or BSAA) anodizing to report an improved short and long-term
393 durability of the produced bonds. The narrow pores close to the substrate are considered to provide the
394 corrosion resistance, while the etched top layer is able to better interlock with the primer/adhesive. In
395 order to avoid over-etching, the time, nature and concentration of the etching solution should be
396 controlled [74]. Such post-anodizing step is not new to the aviation industry, which frequently applies
397 post- anodizing immersion in boiling water to seal the porous oxide layer when it serves as a protective
398 coating against corrosion instead of a receptive surface for bonding.

399 An interesting alternative to a post-treatment dip concerns anodizing combining positive and
400 small-negative voltages. The negative charge at the end of the normal anodizing cycle leads to
401 dissolution of the oxide by hydrogen ions attracted to the temporary negative pole [75]. In this case, the
402 dissolution is done in the same bath as anodizing, reducing the need for an extra processing and rinsing
403 bath.

404 ## 4.6 Non-anodizing processes

405 As previously mentioned, immersion in hot water is often used to seal off the anodic pores. Treatment in
406 boiling water (and even water at 40 and 50 °C, [76]) leads to hydration of the present Al_2O_3 and to the
407 formation of a pseudoboehmite (AlOOH) oxide. Although sealing the pores openings is not desired from
408 a bonding perspective, boiling water treatment has been suggested as a stand-alone treatment to replace
409 anodizing. The hydrated form of oxide has been reported to provide many benefits, besides it being an
410 inexpensive alternative: a highly-porous morphology with a large surface area [77], increased number of
411 surface hydroxyl groups [78] and a low contact angle [79]. Oxide morphology will depend on the
412 temperature and the duration of the treatments. Three representative morphologies are presented in Fig.
413 9. After just 30 s of immersion the surface oxide exhibits a cellular structure with thin ridges (approx. 10
414 nm wide) that provide large porosity. As the treatment time is extended, cell walls develop into distinct
415 plates (of increased thickness) that are oriented normal to the surface. When the time is extended up to 4
416 hours, the cell walls significantly thickness, producing a distinctive and much less porous structure [80].
417 Unfortunately, this type of oxide is brittle and mechanical tests often show an early cohesive failure
418 within this pseudoboehmite layer [77, 79]. Although in some cases, the combination of prior grit blasting
419 and the addition of a silane layer was shown to reproduce results comparable to the benchmark used
420 (CSA+PAA), its level of success is highly sensitive to alloy composition [80]. Hence, boiling water
421 treatment generally does not compare with the durability of anodized-based oxide layers.

422 **Figure 9** High-resolution SEM micrograph after boiling water treatment on AA2024-T3 clad for 30 s (a), 60 min (b) and
423 240 min (c), edited from [80].

424 A similar option consists of a steam treatment [81, 82]. A study by Ud Din et al. [83] have shown that
425 oxide layers with thicknesses comparable to anodic oxides can be produced. Depending on treatment
426 parameters and steam chemistry, layers of few nanometers up to 3 μm can be formed. The addition of
427 acidic components (citric or phosphoric acids) to the steam enables the growth of thicker layers and help
428 in the corrosion protection (especially due to incorporation of phosphates).

429 ## 5. Parameters affecting the anodic oxide film properties

430 Considering the list of alternative methods in section 4, it appears that most processes are based on
431 similar electrolytes that apply different preparation conditions to produce certain desired oxide
432 properties. Hence, it is important to understand which key parameters control the anodizing process and
433 how these, in turn, change the oxide film characteristics.
434

435 ## 5.1 Electrolyte type

436 The nature of the electrolyte is one of the main parameters to determine the oxide properties, such as
437 morphology and chemistry (as discussed in section 5.2). The pore size is a direct function of the

13

438 electrolyte as found by Keller et al. [84]. Interpore distance and barrier layer thickness are also affected,
439 but to a lesser degree. The pore size generally increases in the order SAA < TSA < CAA< < PSA< PAA
440 [85].

441 ## 5.2 Incorporation of anions

442 Besides the ionic species (Al^{3+} and O^{2-}/OH^-) that are responsible for oxide growth, any ion species that is
443 present in the solution may be affected by the electric field. Since the anode is positively charged during
444 anodizing, negatively charged species from dissociating acids will migrate towards the oxide, leading to
445 the incorporation of impurities into the oxide. The extent of incorporation is determined by the nature of
446 the electrolyte solution, the applied conditions and the film type. A range of surface analysis techniques,
447 including Auger electron spectroscopy (AES), X-ray photoelectron spectroscopy (XPS) and glow
448 discharge optical emission spectroscopy (GDOES) [86, 87] have been applied to measure the
449 concentration and distribution of electrolyte-derived impurities in the film. These studies show that the
450 migration of electrolyte species varies from one electrolyte to the other. Table 2 lists the concentration of
451 anions within the most common anodizing electrolytes. It demonstrates that almost anion-free films are
452 formed in chromic acid, while other anions of alternative electrolytes contribute to a much higher relative
453 composition. Since most electrolyte anions migrate at slower rates than the O^{2-} ions, a relatively pure
454 alumina region is formed close to the aluminum/oxide interface [88]. This is indicated in Fig. 10 that
455 displays a comparison of the resulting oxide composition in SAA and PAA. Sulfate anions can migrate
456 into the inner most part of the cell wall, resulting in a duplex oxide composition. Phosphate anions, on
457 the other hand, exhibit a triplex structure with maximal concentration in the region near the interface
458 with the electrolyte. In the mixed PSA (Phosphoric- sulfuric acid anodizing) electrolyte, the
459 incorporation of phosphate on *barrier-type* oxide indicated that the phosphate incorporation in the mixed
460 electrolyte is somewhat inhibited, and phosphates remained close to the oxide/resin interface [58].

461

462

Table 2: Percentage of incorporated anions in the porous oxide layer [85].

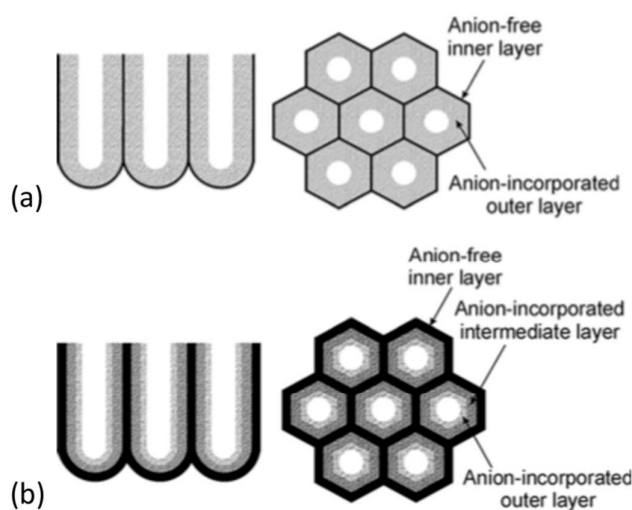| Electrolyte	H_2CrO_4	H_3PO_4	$H_2C_2O_4$	H_2SO_4
Anion concentration (at.%)	$0.1 - 0.3$	6 - 8	2 - 3	10 - 13

463

464 **Figure 10**: Schematic representations of the sectional and plan views of, respectively, the duplex (a) and triplex (b)
465 structures of porous alumina cell walls formed in sulfuric and phosphoric acids, respectively [85].

14

466 Compared to barrier layers, porous film generally contain a higher anion content in the oxide structure
467 [85]. This is explained by the fact that the electric field at the barrier layer is not uniform, so that the
468 semi-spherical shape of the pore base results in a much higher electric field close to the electrolyte/oxide
469 interface, which in turn supports easier incorporation of anions. In addition, the long-term exposure of
470 the oxide walls to the electrolyte readily allows for active penetration of the acid.

471 Anion incorporation has an effect on the properties of the oxide film, such as the mechanical (e.g.
472 flexibility and hardness) the chemical properties and the space charge [89]. Thompson and Wood [90]
473 reported a transition from solid to gel-like material moving across the cell walls towards the pore interior,
474 with the thickness of this layer depending on the electrolyte, the voltage or current density, and the
475 temperature. Another example is the resistance to hydration that is provided by oxides produced in
476 phosphoric acid. This resistance has been contributed to the presence of $H_2PO_4^-$ ions in the anodic films.
477 These anions can be further decomposed to proton, H^+, and HPO_4^{2-}, thereby retarding the hydration of
478 alumina [68]. The applied electrolyte also seems to have an influence on the water content of the film.
479 Although no water is found in the bulk of oxides formed in acid electrolytes, chemical adsorption
480 (chemisorption) of OH^- groups and water molecules at the outer layer is reported [91]. This can,
481 according to findings on chemically grown aluminum oxides, affect the extent in which the oxide interact
482 with organic molecules and resins [92].

483 In a recent publication by the authors [58] we have quantified the relative amount of O^{2-}, OH^-, PO_4^{3-} and
484 SO_4^{2-} species at the surface of *barrier-type* PAA, SAA, PSA and CAA oxides using X-ray photoelectron
485 spectroscopy (XPS). Results show that the surface chemistry of anodic oxides is highly affected by the
486 incorporation of anions. Phosphates were the highest with 40 % of the surface species and no hydroxyls
487 at the applied conditions. Sulfate concentration is lower at 15 % and a negligible amount of anions in
488 CAA. It was confirmed that the incorporation of phosphate and sulfate anions comes at the expense of
489 surface hydroxyls. Consequentially, we investigated how variations in the chemical species at the oxide
490 surface after anodizing affect the interaction with an organic resin. In the first instate, this was studied
491 using molecules that represent typical aerospace adhesives. Results show that bonding with two
492 phenol-based molecules and amine molecule both proceeds through the surface hydroxyls. However,
493 interactions with some molecules were sensitive to chemical changes while others did not. Next,
494 mechanical peel tests with barrier-type anodic oxides that were bonded with an industrial epoxy
495 adhesive. We concluded that the bonding mechanism was not affected by anion incorporation, only its
496 extent. Since phosphate and sulfate incorporation reduces the amount of hydroxyls available for
497 interactions, anodizing in these electrolytes was considered inferior from a chemical interactions point of
498 view [93].

499

500 ## 5.3 Potential / current density

501 At steady state growth, a dynamic equilibrium exists between pore base dissolution at the
502 oxide/electrolyte interface and oxide growth at the metal/oxide interface. Studies have shown that the
503 major film characteristics (pore diameter *d*, cell diameter *c* and barrier layer thickness *b*, as indicated in
504 Fig. 11) are directly related to the applied potential [84, 94]. This is explained by the fact that stationary
505 film formation occurs at a constant rate, which is determined by the average field over the oxide [95].
506 Higher potential values will result in thicker barrier layers, larger cells, and wider pores. The thickening
507 of the barrier layer was found to show an almost universal relation, growing at 1.3-1.4 nm/V for

15

508 barrier-type films and about 1.2 nm/V for the barriers under porous films, with only small deviations as a
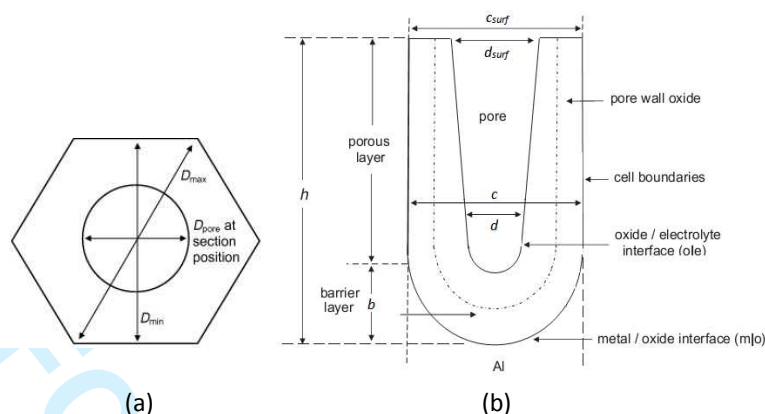509 function of the temperature and the electrolyte type [85].

508 ...

Figure 11: Schematic representation of an ideally hexagonal columnar cell of a porous anodic alumina film [95].

510

511

512 Any tendency of a pore to become too big or too small will be compensated by its curvature that will,
513 accordingly, adjust field strength [96]. If during the anodizing process, a large variation in potential is
514 induced, the oxide film will adapt itself to the new applied conditions. This observations, together with a
515 'recovery effect' was reported by Curioni et al. [97], using cyclic polarization measurements. The
516 recovery effect is the elapsed time before the steady-state characteristic conditions of the new voltage are
517 attained. It will depend on the potential variance, as well as the bath conditions (electrolyte, temperature).
518 Dynamically varying the anodizing potential during the treatment was used by van Put et al. [65] in order
519 to change the pore size across the oxide thickness, creating complex oxide morphologies. This may
520 explain the gradient of voltage that is applied during the conventional 40/50V CAA anodizing process,
521 providing wider pores at the bottom of the film and thickening the barrier layer. This is an interesting
522 observation that can be used as opportunity in developing new processes.

523

524 5.4 Temperature and time

525 Another significant variable in the anodizing conditions is the electrolyte temperature. A higher bath
526 temperature will enhance local dissolution at the pore base. This, in turn, will result in an increased local
527 current density, which will increase the ionic transfer and oxide formation rates [98]. Aerts et al. [99]
528 have shown that a higher rate of oxide dissolution, due to the aggressiveness of the electrolyte at higher
529 temperatures, have increased the porosity in sulfuric acid anodizing (with a constant convection) from
530 4% at 5℃ to 32% at 55℃. Dissolution effects are mainly noticeable at the outer layer of the oxide,
531 leading to pore broadening [100]. Upon extended anodizing times, aggressive electrolytes will cause
532 excessive chemical dissolution. Since the oxide is only growing from within the metal, the outer part of
533 the film is in contact with the electrolyte for a longer time period and therefore suffers from the most
534 chemical attack. This phenomenon induces pore widening at the outer surface, which affects the general
535 shape of the pores. This is why cone-shaped pores are often reported; with the pore diameter at the pore
536 base (d in Fig. 11 (b)) generally exhibiting a linear correlation to the anodizing voltage, while pores at the
537 surface (d_{surf} in Fig. 11 (b)) are frequently larger [59]. Interestingly, controlling the electrode temperature
538 can have a larger influence on oxide formation than changing the electrolyte temperature [101]. Hence,
539 physical bath properties, such as convection-based heat transfer should be considered.

16

540 At high anodizing temperatures and longer times, dissolution has an even larger influence on oxide
541 morphology. An example is shown in Fig. 12 for different electrolyte temperatures and dwell time. At
542 relatively lower temperatures and shorter times whiskers are formed on top of the hexagonal oxide
543 structure. These are created by extended dissolution and thinning of the pore walls. At some critical
544 point, these filaments are so long and thin, that they will collapse, forming a so-called 'bird's nest'
545 structure on top of the oxide film (Fig. 12 m-o).
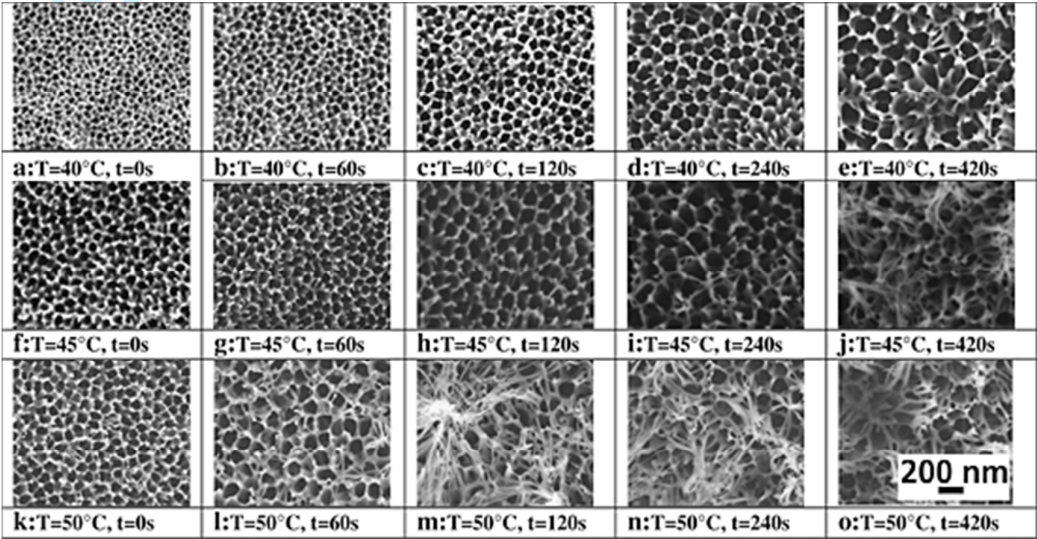546

547
548 **Figure 12:** SEM of the oxide layer depending on the bath temperature and the dwell time - surface views (anodizing
549 potential E = 50 VSCE) [102]. Longer time and higher temperatures lead to their collapse and the formation of a 'bird's
550 nest'.
551

552 5.5 Pre-texturing

553 Studies have shown that surface features produced by prior steps are related to pore initiation and
554 development. Following the previously discussed growth mechanism, geometrical (near-)surface features
555 like the rolling lines, scratches and rolled-in oxides locally increase the curvature and therefore present
556 preferential regions for pore initiation and development. It has been shown by Terryn [103] that such
557 features can even pre-impose the alignment of pores to develop certain orientation. This is especially
558 relevant when the step prior to anodizing produces characteristic surface features. If a highly-regular pore
559 arrangement is required, as in the production of alumina template for nanostructure fabrication, a
560 two-step anodizing (with intermediate dissolution of the oxide) is used to produce a well-ordered
561 structure, in which the first anodizing step is used to texture the surface [85]. Since this method is both
562 time-consuming and expensive, pre-texturing by anodizing is generally not applied in the aerospace
563 industry.

564 5.6 Alloy composition

565 The presence of alloying elements has an effect on the anodizing potential, as well as the oxide
566 morphology. Since elements in solid solution will change the resistance to current flow, the purer the
567 aluminum, the more resistance to ionic transport [104].

17

568 It is generally also observed that the same process conditions can yield completely different forms of
569 anodic films on bare and clad aluminum substrates. Fig. 13 shows a comparison between the CAA
570 40/50V anodic oxide on clad and bare AA20204-T3. The high purity clad alloy shows a relatively
571 regular columnar structure while no evidently regular structure is observed on the bare material, which
572 resembles a sponge-like structure. This difference is attributed to the presence of second phase particles
573 and alloying elements with a different potential than that of the matrix [69, 105, 106]. Alloying elements
574 with more negative potential will oxidize with aluminum and enter the anodic oxide, while nobler
575 alloying elements like Cu do not. Cu concentration will then rise, leading to enrichment at the
576 metal/oxide interface, immediately beneath the oxide film [107, 108]. It has been shown by
577 Garcia-Vergara et.al [109] that cyclic oxidation of copper in the enriched layer below the barrier layer
578 results in oxygen generation that leads to gas evolution and lateral porosity, resulting in the irregular
579 anodic oxide structure that is produced on bare A2024-T3. Correspondingly, similar process conditions
580 may lead to different oxide weight and morphology on different aluminum alloys.

581 **Figure 13**: CAA 40/50 V processed, 2024-T3 bare: plan view (a) and cross-section (b), 2024-T3 clad: plan view (c) and
582 cross-section (d). Reprinted from [69], Copyright (2016), with permission from Elsevier.

583 # 6. The relation between oxide properties and adhesion

584 The two main oxide properties that are influenced by the different process parameters are oxide
585 composition and morphological features. Yet, it appears that the main objective in the development of
586 Cr(VI)-free processes so far was to reproduce the CAA morphological features using different types of
587 processes. One of the longest, yet, on-going discussions in the literature concern the adhesion modes.
588 Various theories exist to explain adhesion between different materials: diffusion, electrostatic
589 interactions, weak boundary layer, mechanical interlocking and physical chemical adsorption (or
590 interactions) [110]. Amongst these theories adsorption and mechanical models are considered most
591 relevant for metal/polymer bonding.

592 Different authors argue that the high level adhesion that is achieved with porous anodic oxides is mainly
593 due to mechanical interlocking [27, 111-113]. However, studies on both chemical and anodic oxides
594 have shown that oxide chemistry also plays a vital role in the nature and type of interaction with the
595 organic resin [92, 114-117]. In an effort to separate the two contributions, a study by the authors using

18

596 FM 73 epoxy adhesive shows that significant initial adhesion strength can be achieved without
597 mechanical interlocking and independent of the type of electrolyte. The measured dry peel strengths were
598 in the same level of the dry strengths measured for porous oxides with a relatively small pore size (up to
599 20 nm). However, porous oxides with wider pores performed better. Above approximately 25 nm pore
600 size, tests showed no further improvement in dry peel strengths [59]. According to these observations, it
601 is not possible to conclude which is the dominating adhesion mechanism. Both mechanical interlocking
602 and a larger contact area could provide this improvement in strength.

603 Conversely, the stability of the interface under water ingress was found to be highly dependent on the
604 oxide chemistry and anodizing conditions, especially the electrolyte type, concentration and temperature.
605 Chemistry effects were correlated to the amount of surface hydroxyls, which were found to be the
606 reacting entities between the oxide and the resin [116], while morphological considerations were mainly
607 attributed to changes in the surface roughness [59]. Nevertheless, bond strength and durability both
608 appear to be closely related to the ability of the oxide and the resin to form a cohesive interphase.
609 Although mechanical interlocking is considered to contribute, there is no conclusive evidence for its
610 dominance.

611 Another important aspect in bond durability is the resistance to bondline corrosion. It appears that
612 increasing the oxide porosity and surface roughness will improve adhesion. However, as also claimed to
613 PAA, one of the main challenges is to provide a high level of corrosion resistance in a very porous
614 system. Consequently, failures due to bondline corrosion were observed with PSA test panels produced
615 at relatively aggressive conditions and lower voltages [59]. Oxides produced in the same conditions
616 (electrolyte, temperature and time), but at higher voltage did not fail. This seems to indicate that the
617 presence of thicker barrier-layer that is formed at higher voltages may be playing a significant role.
618 Furthermore, this is the reason why many studies combine the production of a receptive open structure at
619 the outer layer, while aiming to provide better corrosion protection by a denser inner layer. Nevertheless,
620 a recent (unpublished) investigation of the authors indicates that the corrosion resistance of the interface
621 is also largely determined by the chemical composition of the adhesive. Hence, the chemical nature of
622 the oxide *and* the adhesive should be considered.

7. Summary and Conclusions

624   The required bond performance and durability, together with the corrosion sensitivity of aerospace
625 aluminum alloys, have led to the development of a multi-step pre-treatment process that is carefully
626 designed to provide the desired surface characteristics for bonding and corrosion resistance. In this
627 pre-treatment, the use of Cr(VI)-based chemistries currently still has a crucial role. The importance of
628 finding a replacement is evident by the large amount of literature available on this subject. It is, however,
629 also clear that the success and versatility of Cr(VI)-based applications is one that is very difficult to
630 duplicate. While many Cr(VI)-free alternative options exist and much is known about the relation
631 between the principal process parameters and oxide properties, maximizing bond performance and
632 corrosion resistance is not straightforward. The fact that both atomic- and molecular interactions, as well
633 as mechanical interlocking are crucial for the formation of interfacial bonds are now beginning to be
634 reflected in practical and industrial research. Hence, it is of pivotal importance to adjust both oxide
635 chemistry and morphology in order to produce the desired oxide characteristics. It remains of great
636 academic and industrial interest to continue to gain further fundamental understanding on how adsorption
637 and mechanical adhesion mechanisms contribute to the final bond performance.

19

638   **8.References**
639   1.   ATSDR. Toxicologica Profile for Chromium. 2012,
640   2.   Sueker J K. 5 - Chromium A2 - Morrison, Robert D. In: Murphy B L, (ed). Environmental
641   Forensics. Burlington: Academic Press, 1964, 81-95
642   3.   Royle H. Toxicity of chromic acid in the chromium plating industry (1). Environmental
643   Research, 1975, 10(1): 39-53
644   4.   Murray R. Health of Workers in Chromate Producing Industry. British Journal of Industrial
645   Medicine, 1957, 14(2): 140-141
646   5.   Alexander B H, Checkoway H, Wechsler L, Heyer N J, Muhm J M, O'Keeffe T P. Lung Cancer
647   in Chromate-Exposed Aerospace Workers. Journal of Occupational and Environmental Medicine, 1996,
648   38(12): 1253-1258
649   6.   Vallero D. Chapter 11 - Cancer and Air Pollutants. Fundamentals of Air Pollution (Fifth
650   Edition). Boston: Academic Press, 2014, 271-311
651   7.   OSHA. Toxic and Hazardous Substances Occupational Exposure to Hexavalent Chromium,
652   2006, 1910.1026(
653   8.   Ebnesajjad S. 1 - Introduction and Adhesion Theories. In: Ebnesajjad S, (ed). Handbook of
654   Adhesives and Surface Preparation. Oxford: William Andrew Publishing, 2011, 3-13
655   9.   Brockmann W, Geiß P L, Klingen J, Schröder B. Adhesive Bonding: Wiley-VCH Verlag
656   GmbH & Co. KGaA, 2009
657   10.   Marshall S J, Bayne S C, Baier R, Tomsia A P, Marshall G W. A review of adhesion science.
658   Dental Materials, 2010, 26(2): e11-e16
659   11.   Bishopp J. Adhesives for Aerospace Structures. In: Ebnesajjad S, (ed). Handbook of
660   Adhesives and Surface Preparation. Oxford: William Andrew Publishing, 2011, 301-344
661   12.   Higgins A. Adhesive bonding of aircraft structures. International Journal of Adhesion and
662   Adhesives, 2000, 20(5): 367-376
663   13.   Sargent J P. Durability studies for aerospace applications using peel and wedge tests.
664   International Journal of Adhesion and Adhesives, 2005, 25(3): 247-256
665   14.   Zanni-Deffarges M P, Shanahan M E R. Diffusion of water into an epoxy adhesive:
666   comparison between bulk behaviour and adhesive joints. International Journal of Adhesion and Adhesives,
667   1995, 15(3): 137-142
668   15.   Posner R, Ozcan O, Grundmeier G. Water and Ions at Polymer/Metal Interfaces. In: Silva M L
669   F, Sato C, (eds). Design of Adhesive Joints Under Humid Conditions. Berlin, Heidelberg: Springer Berlin
670   Heidelberg, 2013, 21-52
671   16.   Sheasby P G, Pinner R. Surface Treatment and Finishing of Aluminium and its Alloys. 6th ed.
672   England: Finishing Publications Ltd., 2001.
673   17.   Sukiman N L, Zhou X, Birbilis N, Hughes A E, Mol J M C, Garcia S J, X. Z, Thompson G E.
674   Durability and Corrosion of Aluminium and Its Alloys: Overview, Property Space, Techniques and
675   Developments. Aluminium Alloys - New Trends in Fabrication and Applications: InTech, 2012, 47- 97
676   18.   Lyle J P, Granger D A, Sanders R E. Aluminum Alloys. Ullmann's Encyclopedia of Industrial
677   Chemistry: Wiley-VCH Verlag GmbH & Co. KGaA, 2000
678   19.   Boag A, Hughes A E, Glenn A M, Muster T H, McCulloch D. Corrosion of AA2024-T3 Part I:
679   Localised corrosion of isolated IM particles. Corrosion Science, 2011, 53(1): 17-26
680   20.   Hughes A E, Boag A, Glenn A M, McCulloch D, Muster T H, Ryan C, Luo C, Zhou X,
681   Thompson G E. Corrosion of AA2024-T3 Part II: Co-operative corrosion. Corrosion Science, 2011, 53(1):
682   27-39

20

683   21.   Glenn A M, Muster T H, Luo C, Zhou X, Thompson G E, Boag A, Hughes A E. Corrosion of
684   AA2024-T3 Part III: Propagation. Corrosion Science, 2011, 53(1): 40-50
685   22.   Afseth A. Norway: NTNU Trondheim, 1999
686   23.   Zhou X, Liu Y, Thompson G E, Scamans G M, Skeldon P, Hunter J A. Near-Surface
687   Deformed Layers on Rolled Aluminum Alloys. Metallurgical and Materials Transactions A, 2011, 42(5):
688   1373-1385
689   24.   Critchlow G W, Brewis D M. Review of surface pretreatments for aluminium alloys.
690   International Journal of Adhesion and Adhesives, 1996, 16(4): 255-275
691   25.   Wegman R F, Van Twisk J. 2 - Aluminum and Aluminum Alloys. In: Wegman R F, Twisk J
692   V, (eds). Surface Preparation Techniques for Adhesive Bonding (Second Edition): William Andrew
693   Publishing, 2013, 9-37
694   26.   Pocius A V. The Electrochemistry of the FPL (Forest Products Laboratory) Process and its
695   Relationship to the Durability of Structural Adhesive Bonds. The Journal of Adhesion, 1992, 39(2-3): 101-121
696   27.   Venables J D, McNamara D K, Chen J M, Sun T S, Hopping R L. Oxide morphologies on
697   aluminum prepared for adhesive bonding. Applications of Surface Science, 1979, 3(1): 88-98
698   28.   Carter E A. High current anodization of magnesium and magnesium alloysThe University of
699   Auckland, 1996
700   29.   Su Z, Zhou W. Porous Anodic Metal Oxides. Science Foundation in China, 2008, 16(1): 36
701   30.   Aerts T. Study of the influence of temperature and heat transfer during anodic oxide growth on
702   aluminiumVrije Universiteit Brussel, 2009
703   31.   Thompson G E. Porous anodic alumina: fabrication, characterization and applications. Thin
704   Solid Films, 1997, 297: 192-201
705   32.   O'Sullivan J P, Wood G C. Morphology and mechanism of formation of porous anodic films
706   on aluminum. Proceedings of the Royal Society of London Series A - Mathematical and Physical Sciences,
707   1970, 317: 511-543
708   33.   Setoh S, Miyata A. Sci. Pap. Inst. Phys. Chem. Res., 1932, 189
709   34.   Keller F, Hunter M S, Robinson D L. Structureal features of oxide coatings on aluminum.
710   Journal of The Electrochemical Society, 1953, 100: 411-419
711   35.   Wernick S, Pinner R, Sheasby P G. The surface treatment and finishing of aluminium and its
712   alloys. 5 ed. Ohio and Middlesex: ASM International and Finishing Publications LTD., 1987
713   36.   Critchlow G W, Yendall K A, Bahrani D, Quinn A, Andrews F. Strategies for the replacement
714   of chromic acid anodising for the structural bonding of aluminium alloys. International Journal of Adhesion
715   and Adhesives, 2006, 26(6): 419-453
716   37.   Brockmann W, Hennemann O D, Kollek H. Surface properties and adhesion in bonding
717   aluminium alloys by adhesives. International Journal of Adhesion and Adhesives, 1982, 2(1): 33-40
718   38.   Oosting R. Toward a new durable and environmentally compliant adhesive bonding process
719   for aluminum alloys. The Netherlands Delft University of Technology, 1995
720   39.   Olsson-Jacques C L, Wilson A R, Rider A N, Arnott D R. Effect of Contaminant on the
721   Durability of Epoxy Adhesive Bonds with Alclad 2024 Aluminium Alloy Adherends. Surface and Interface
722   Analysis, 1996, 24(9): 569-577
723   40.   Kinloch A J, Little M S G, Watts J F. The role of the interphase in the environmental failure of
724   adhesive joints. Acta Materialia, 2000, 48(18–19): 4543-4553
725   41.   G. Pape P. 15 - Adhesion Promoters. In: Ebnesajjad S, (ed). Handbook of Adhesives and
726   Surface Preparation. Oxford: William Andrew Publishing, 2011, 369-386

21

727   42.   Abel M-L, Digby R P, Fletcher I W, Watts J F. Evidence of specific interaction between
728   γ-glycidoxypropyltrimethoxysilane and oxidized aluminium using high-mass resolution ToF-SIMS. Surface
729   and Interface Analysis, 2000, 29(2): 115-125
730   43.   Tchoquessi Doidjo M R, Belec L, Aragon E, Joliff Y, Lanarde L, Meyer M, Bonnaudet M,
731   Perrin F X. Influence of silane-based treatment on adherence and wet durability of fusion bonded epoxy/steel
732   joints. Progress in Organic Coatings, 2013, 76(12): 1765-1772
733   44.   Ooij W, Zhu D, Palanivel V, Lamar J A, Stacy M. Overview: The Potential of silanes for
734   chromate replacement in metal finishing industries. Silicon Chemistry, 2006, 3(1-2): 11-30
735   45.   Thiedmanu W, Tolan F C, Pearce P J, Morris C E M. Silane Coupling Agents as Adhesion
736   Promoters for Aerospace Structural Film Adhesives. The Journal of Adhesion, 1987, 22(3): 197-210
737   46.   Cabral A, Duarte R G, Montemor M F, Zheludkevich M L, Ferreira M G S. Analytical
738   characterisation and corrosion behaviour of bis-[triethoxysilylpropyl]tetrasulphide pre-treated AA2024-T3.
739   Corrosion Science, 2005, 47(3): 869-881
740   47.   Cabral A M, Duarte R G, Montemor M F, Ferreira M G S. A comparative study on the
741   corrosion resistance of AA2024-T3 substrates pre-treated with different silane solutions: Composition of the
742   films formed. Progress in Organic Coatings, 2005, 54(4): 322-331
743   48.   Song J, Van Ooij W J. Bonding and corrosion protection mechanisms of γ-APS and BTSE
744   silane films on aluminum substrates. Journal of Adhesion Science and Technology, 2003, 17(16): 2191-2221
745   49.   Franquet A, Terryn H, Vereecken J. Study of the effect of different aluminium surface
746   pretreatments on the deposition of thin non-functional silane coatings. Surface and Interface Analysis, 2004,
747   36(8): 681-684
748   50.   Park S Y, Choi W J, Choi H S, Kwon H, Kim S H. Recent Trends in Surface Treatment
749   Technologies for Airframe Adhesive Bonding Processing: A Review (1995–2008). The Journal of Adhesion,
750   2010, 86(2): 192-221
751   51.   Hughes A E, Cole I S, Muster T H, Varley R J. Designing green, self-healing coatings for
752   metal protection. NPG Asia Mater, 2010, 2: 143-151
753   52.   Marceau J A, Firminhac R H, Moji Y. Method for providing environmentally stable aluminum
754   surfaces for adhesive bonding and product produced. 1978,
755   53.   Kinloch A J, Welch L S, Bishop H E. The Locus of Environmental Crack Growth in Bonded
756   Aluminium Alloy Joints. The Journal of Adhesion, 1984, 16(3): 165-177
757   54.   Visser P, Terryn H, Mol J M. Aerospace Coatings. In: Hughes A E, Mol J M C, Zheludkevich
758   M L, Buchheit R G, (eds). Active Protective Coatings: Springer, 2016, 315-372
759   55.   Sulka G D, Parkoła K G. Temperature influence on well-ordered nanopore structures grown by
760   anodization of aluminium in sulphuric acid. Electrochimica Acta, 2007, 52(5): 1880-1888
761   56.   Arrowsmith D J, Clifford A W. Morphology of anodic oxide for adhesive bonding of
762   aluminum. International Journal of Adhesion and Adhesives, 1983, 3(4): 193-196
763   57.   Kock E, Muss V, Matz C, De wit F. Verfahren zur anodischen oxidation. 1993, EP0607579
764   A1(
765   58.   Abrahami S T, Hauffman T, de Kok J M M, Mol J M C, Terryn H. XPS Analysis of the
766   Surface Chemistry and Interfacial Bonding of Barrier-Type Cr(VI)-Free Anodic Oxides. The Journal of
767   Physical Chemistry C, 2015, 119(34): 19967-19975
768   59.   Abrahami S T, de Kok J M M, Gudla V C, Ambat R, Terryn H, Mol J M C. Interface Strength
769   and Degradation of Adhesively Bonded Porous Aluminum Oxides npj Materials Degradation, 2017, accepted
770   60.   Kape J M. Electroplating Met. Finish., 1961, 11: 407-415

22

771   61.   Curioni M, Skeldon P, Koroleva E, Thompson G E, Ferguson J. Role of Tartaric Acid on the
772   Anodizing and Corrosion Behavior of AA 2024 T3 Aluminum Alloy. Journal of the Electrochemical Society,
773   2009, 156(4): C147-C153
774   62.   García-Rubio M, de Lara M P, Ocón P, Diekhoff S, Beneke M, Lavía A, García I. Effect of
775   postreatment on the corrosion behaviour of tartaric–sulphuric anodic films. Electrochimica Acta, 2009, 54(21):
776   4789-4800
777   63.   García-Rubio M, Ocón P, Climent-Font A, Smith R W, Curioni M, Thompson G E, Skeldon P,
778   Lavía A, García I. Influence of molybdate species on the tartaric acid/sulphuric acid anodic films grown on
779   AA2024 T3 aerospace alloy. Corrosion Science, 2009, 51(9): 2034-2042
780   64.   Kock E. Design of a novel anodic film to meet the requirements of aircraft applications. In:
781   *Proceedings of* 2004, Bremen, Germany
782   65.   van Put M, Abrahami S T, Elisseeva O, de Kok J M M, Mol J M C, Terryn H.
783   Potentiodynamic anodizing of aluminum alloys in Cr(VI)-free electrolytes. Surface and Interface Analysis,
784   2016, 48(8): 946-952
785   66.   Boeing. Process Spec. Boric Acid -- Sulfuric Acid Anodizing, Revision D. 2004, BAC 5632(
786   67.   Domingues L, Fernandes J C S, Da Cunha Belo M, Ferreira M G S, Guerra-Rosa L. Anodising
787   of Al 2024-T3 in a modified sulphuric acid/boric acid bath for aeronautical applications. Corrosion Science,
788   2003, 45(1): 149-160
789   68.   Zhang J-s, Zhao X-h, Zuo Y, Xiong J-p. The bonding strength and corrosion resistance of
790   aluminum alloy by anodizing treatment in a phosphoric acid modified boric acid/sulfuric acid bath. Surface
791   and Coatings Technology, 2008, 202(14): 3149-3156
792   69.   Yendall K A, Critchlow G W. Novel methods, incorporating pre- and post-anodising steps, for
793   the replacement of the Bengough–Stuart chromic acid anodising process in structural bonding applications.
794   International Journal of Adhesion and Adhesives, 2009, 29(5): 503-508
795   70.   Bjørgum A, Lapique F, Walmsley J. AC anodising as pre-treatment prior to adhesive bonding
796   of aluminium. 2004,
797   71.   Critchlow G W, Yendall K A, Lu J. Friendlier Surface Treatments – For Metals. Society for
798   Adhesion and Adhesives in conjunction with BASA, 2007,
799   72.   Critchlow G, Ashcroft I, Cartwright T, Bahrani D. Anodising aluminum alloy. 2011,
800   73.   Arrowsmith D J, Clifford A W. A new pretreatment for the adhesive bonding of aluminium.
801   International Journal of Adhesion and Adhesives, 1985, 5(1): 40-42
802   74.   Digby R P, Packham D E. Pretreatment of aluminium: topography, surface chemistry and
803   adhesive bond durability. International Journal of Adhesion and Adhesives, 1995, 15(2): 61-71
804   75.   Chung C K, Liao M W, Chang H C, Lee C T. Effects of temperature and voltage mode on
805   nanoporous anodic aluminum oxide films by one-step anodization. Thin Solid Films, 2011, 520(5): 1554-1558
806   76.   Underhill P R, Rider A N. Hydrated oxide film growth on aluminium alloys immersed in warm
807   water. Surface and Coatings Technology, 2005, 192(2–3): 199-207
808   77.   Rider A N. The influence of porosity and morphology of hydrated oxide films on
809   epoxy-aluminium bond durability. Journal of Adhesion Science and Technology, 2001, 15(4): 395-422
810   78.   Özkanat Ö, Salgin B, Rohwerder M, Mol J M C, de Wit J H W, Terryn H. Scanning Kelvin
811   Probe Study of (Oxyhydr)oxide Surface of Aluminum Alloy. The Journal of Physical Chemistry C, 2011,
812   116(2): 1805-1811
813   79.   Özkanat Ö, de Wit F M, de Wit J H W, Terryn H, Mol J M C. Influence of pretreatments and
814   aging on the adhesion performance of epoxy-coated aluminum. Surface and Coatings Technology, 2013,
815   215(0): 260-265

23

816   80.   Rider A N, Arnott D R. Boiling water and silane pre-treatment of aluminium alloys for durable
817   adhesive bonding. International Journal of Adhesion and Adhesives, 2000, 20(3): 209-220

818   81.   Din R U, Piotrowska K, Gudla V C, Jellesen M S, Ambat R. Steam assisted oxide growth on
819   aluminium alloys using oxidative chemistries: Part I Microstructural investigation. Applied Surface Science,
820   2015, 355: 820-831

821   82.   Din R U, Jellesen M S, Ambat R. Steam assisted oxide growth on aluminium alloys using
822   oxidative chemistries: Part II corrosion performance. Applied Surface Science, 2015, 355: 716-725

823   83.   Din R U, Jellesen M S, Ambat R. Role of acidic chemistries in steam treatment of aluminium
824   alloys. Corrosion Science, 2015, 99: 258-271

825   84.   Keller F, Hunter M S, Robinson D L. Structural Features of Oxide Coatings on Aluminum.
826   Journal of the Electrochemical Society, 1953, 100(9): 411-419

827   85.   Sulka G D. Highly Ordered Anodic Porous Alumina Formation by Self-Organized Anodizing.
828   Nanostructured Materials in Electrochemistry: Wiley-VCH Verlag GmbH & Co. KGaA, 2008, 1-116

829   86.   Parkhutik V P. The initial stages of aluminium porous anodization studied by Auger electron
830   spectroscopy. Corrosion Science, 1986, 26(4): 295-310

831   87.   Xu Y, Thompson G E, Wood G C, Bethune B. Anion incorporation and migration during
832   barrier film formation on aluminium. Corrosion Science, 1987, 27(1): 83-102

833   88.   González-Rovira L, López-Haro M, Hungría A B, El Amrani K, Sánchez-Amaya J M, Calvino
834   J J, Botana F J. Direct sub-nanometer scale electron microscopy analysis of anion incorporation to self-ordered
835   anodic alumina layers. Corrosion Science, 2010, 52(11): 3763-3773

836   89.   Ono S, Ichinose H, Masuko N. The high resolution observation of porous anodic films formed
837   on aluminum in phosphoric acid solution. Corrosion Science, 1992, 33(6): 841-850

838   90.   Thompson G E, Wood G C. 5 - Anodic Films on Aluminium. In: J.C S, (ed). Treatise on
839   Materials Science and Technology: Elsevier, 1983, 205-329

840   91.   Alexander M R, Thompson G E, Beamson G. Characterization of the oxide/hydroxide surface
841   of aluminium using x-ray photoelectron spectroscopy: a procedure for curve fitting the O 1s core level.
842   Surface and Interface Analysis, 2000, 29(7): 468-477

843   92.   van den Brand J, Blajiev O, Beentjes P C J, Terryn H, de Wit J H W. Interaction of Anhydride
844   and Carboxylic Acid Compounds with Aluminum Oxide Surfaces Studied Using Infrared Reflection
845   Absorption Spectroscopy. Langmuir, 2004, 20(15): 6308-6317

846   93.   Abrahami S T, Hauffman T, de Kok J M M, Mol J M C, Terryn H. Effect of Anodic
847   Aluminum Oxide Chemistry on Adhesive Bonding of Epoxy. The Journal of Physical Chemistry C, 2016,
848   Accepted for publication

849   94.   Wood G C, O'Sullivan J P. The anodizing of aluminium in sulphate solutions. Electrochimica
850   Acta, 1970, 15(12): 1865-1876

851   95.   Patermarakis G, Moussoutzanis K. Transformation of porous structure of anodic alumina films
852   formed during galvanostatic anodising of aluminium. Journal of Electroanalytical Chemistry, 2011, 659(2):
853   176-190

854   96.   Thompson G E. Porous anodic alumina: fabrication, characterization and applications. Thin
855   Solid Films, 1997, 297(1–2): 192-201

856   97.   Curioni M, Skeldon P, Thompson G E. Anodizing of Aluminum under Nonsteady Conditions.
857   Journal of the Electrochemical Society, 2009, 156(12): C407-C413

858   98.   Han X Y, Shen W Z. Improved two-step anodization technique for ordered porous anodic
859   aluminum membranes. Journal of Electroanalytical Chemistry, 2011, 655(1): 56-64

24

860   99.   Aerts T, Dimogerontakis T, De Graeve I, Fransaer J, Terryn H. Influence of the anodizing
861   temperature on the porosity and the mechanical properties of the porous anodic oxide film. Surface and
862   Coatings Technology, 2007, 201(16–17): 7310-7317

863   100.   Stępniowski W J, Bojar Z. Synthesis of anodic aluminum oxide (AAO) at relatively high
864   temperatures. Study of the influence of anodization conditions on the alumina structural features. Surface and
865   Coatings Technology, 2011, 206(2-3): 265-272

866   101.   Aerts T, Jorcin J-B, De Graeve I, Terryn H. Comparison between the influence of applied
867   electrode and electrolyte temperatures on porous anodizing of aluminium. Electrochimica Acta, 2010, 55(12):
868   3957-3965

869   102.   Schneider M, Kremmer K, Weidmann S K, Fürbeth W. Interplay between parameter variation
870   and oxide structure of a modified PAA process. Surface and Interface Analysis, 2013, 45(10): 1503-1509

871   103.   Terryn H. Electrochemical investigation of AC electrograining of aluminium and its porous
872   anodic oxidation. Brussel: Vrije Universiteit Brussel, 1987

873   104.   Zaraska L, Sulka G D, Szeremeta J, Jaskuła M. Porous anodic alumina formed by anodization
874   of aluminum alloy (AA1050) and high purity aluminum. Electrochimica Acta, 2010, 55(14): 4377-4386

875   105.   Curioni M, Scenini F. The Mechanism of Hydrogen Evolution During Anodic Polarization of
876   Aluminium. Electrochimica Acta, 2015, 180: 712-721

877   106.   Curioni M, Saenz de Miera M, Skeldon P, Thompson G E, Ferguson J. Macroscopic and
878   Local Filming Behavior of AA2024 T3 Aluminum Alloy during Anodizing in Sulfuric Acid Electrolyte.
879   Journal of the Electrochemical Society, 2008, 155(8): C387-C395

880   107.   Schneider M, Yezerska O, Lohrengel M M. Anodic oxide formation on AA2024:
881   electrochemical and microstructure investigation. Corrosion Engineering, Science and Technology, 2008,
882   43(4): 304-312

883   108.   Saenz de Miera M, Curioni M, Skeldon P, Thompson G E. The behaviour of second phase
884   particles during anodizing of aluminium alloys. Corrosion Science, 2010, 52(7): 2489-2497

885   109.   Garcia-Vergara S J, El Khazmi K, Skeldon P, Thompson G E. Influence of copper on the
886   morphology of porous anodic alumina. Corrosion Science, 2006, 48(10): 2937-2946

887   110.   Kollek H. Some aspects of chemistry in adhesion on anodized aluminium. International
888   Journal of Adhesion and Adhesives, 1985, 5(2): 75-80

889   111.   Packham D E. Surface energy, surface topography and adhesion. International Journal of
890   Adhesion and Adhesives, 2003, 23(6): 437-448

891   112.   Packham D E, Johnston C. Mechanical adhesion: were McBain and Hopkins right? An
892   empirical study. International Journal of Adhesion and Adhesives, 1994, 14(2): 131-135

893   113.   Allen K W. Some reflections on contemporary views of theories of adhesion. International
894   Journal of Adhesion and Adhesives, 1993, 13(2): 67-72

895   114.   van den Brand J, Blajiev O, Beentjes P C J, Terryn H, de Wit J H W. Interaction of Ester
896   Functional Groups with Aluminum Oxide Surfaces Studied Using Infrared Reflection Absorption
897   Spectroscopy. Langmuir, 2004, 20(15): 6318-6326

898   115.   Özkanat Ö, Salgin B, Rohwerder M, Wit J, Mol J, Terryn H. Interactions at
899   polymer/(oxyhydr) oxide/aluminium interfaces studied by Scanning Kelvin Probe. Surface and Interface
900   Analysis, 2012, 44(8): 1059-1062

901   116.   Abrahami S T, Hauffman T, de Kok J M M, Mol J M C, Terryn H. Effect of Anodic
902   Aluminum Oxide Chemistry on Adhesive Bonding of Epoxy. The Journal of Physical Chemistry C, 2016,
903   120(35): 19670-19677

25

904   117.   Abrahami S T, Hauffman T, de Kok J M M, Terryn H, Mol J M C. The role of acid-base
905   properties in the interactions across the oxide-primer interface in aerospace applications. Surface and Interface
906   Analysis, 2016, 48(8): 712-720

907

26